STRUCTURE AND MECHANISM OF DNA POLYMERASES

By PAUL J. ROTHWELL AND GABRIEL WAKSMAN

Institute of Structural Molecular Biology, University College London and Birkbeck College, Malet Street, London WC1E 7HX, United Kingdom

I. Introduction 402
II. Biological Diversity of DNA Polymerases 403
A. Family A 403
B. Family B 403
C. Family C 404
D. Family D 404
E. Family X 404
F. Family Y 405
G. RT Family 406
III. The Nucleotide Incorporation Pathway 406
A. General Theme 406
B. Variation on a Theme 408
IV. The E State: Basic Architecture of DNA Polymerases 409
V. Primer/Template DNA Binding and Recognition 414
VI. Formation of the E:p/t:dNTP Complex 417
VII. Conformational Transition to a Catalytically Active Ternary Complex: The E':p/t:dNTP Complex 419
A. Structures of E':p/t:ddNTP Complexes 420
B. Molecular Basis for the Rate-Limiting Step 423
C. Discrimination Between Correct Versus Incorrect Nucleotide 426
VIII. Phosphoryl Transfer Reaction, Product Release, and Translocation of the Primer/Template DNA 428
A. Phosphoryl Transfer Reaction and Product Release 428
B. Translocation of Primer/Template DNA 429
C. Force Generation: DNA Polymerases as Molecular Motors 429
IX. Conclusion 430
References 431

Abstract

DNA polymerases are molecular motors directing the synthesis of DNA from nucleotides. All polymerases have a common architectural framework consisting of three canonical subdomains termed the *fingers, palm,* and *thumb* subdomains. Kinetically, they cycle through various states corresponding to conformational transitions, which may or may not generate force. In this review, we present and discuss the kinetic, structural, and single-molecule works that have contributed to our understanding of DNA polymerase function.

ADVANCES IN PROTEIN CHEMISTRY, Vol. 71
DOI: 10.1016/S0065-3233(04)71011-6

Copyright 2005, Elsevier Inc.
All rights reserved.

0065-3233/05 $35.00

I. Introduction

The viability of an organism is dependent on the accurate replication of its genome. In general, this is performed with only one error generated for every 10^9–10^{10} bases replicated (Echols and Goodman, 1991). This remarkable accuracy is achieved by a combination of different mechanisms working in unison. The initial discrimination is carried out during the nucleotide incorporation stage in which a DNA polymerase accurately selects a nucleotide (2'-deoxyribonucleoside-5'-triphosphate (dNTP)) to be added to a primer strand of a duplex DNA, based on its complementarity to a template base provided by a template strand of DNA. In the event of the wrong nucleotide being inserted, this can be removed by the actions of 3'-5' exonucleases. In the case of an error being ''sealed'' into the genome by incorporation of dNTPs past the site of an error, replicative excision/repair pathways exist to remove the offending base. The highest contribution to accuracy is provided by the DNA polymerase activity.

Various models have been proposed by which DNA polymerases select the correct nucleotide from a pool of structurally similar nucleotides. The initial idea, proposed by Watson and Crick (1953a,b) based on the structure of DNA, was that selection could be determined by the A-T and G-C hydrogen bond–mediated base pairing. However, replicative polymerases have error rates for nucleotide insertion in the range of 10^{-3}–10^{-6}/base replicated and the difference in energy between correct versus incorrect base pairs would, at best, only account for an error frequency of 2×10^{-2} (Loeb and Kunkel, 1982). The polymerase, therefore, must be performing a more active role, rather than providing a platform for zipping DNA. A second model proposed that DNA polymerases select correct over incorrect nucleotides due to base pair geometry (Bruskov and Poltev, 1979; Engel and von Hippel, 1978; Sloane *et al.*, 1988). In this case, the shape of the DNA polymerase active site is such that a correct Watson-Crick (W-C) base pair could be accommodated, whereas a non-W-C base pair would be rejected. It has also been proposed that free energy differences between correct versus incorrect base pairs could be amplified due to exclusion of water molecules in the polymerase active site (Petruska *et al.*, 1986).

This chapter will review the current understanding of the nucleotide incorporation cycle by DNA polymerases and the mechanisms employed by DNA polymerases to replicate DNA accurately. It includes a review of more recent and stimulating work that explores the mechanochemistry of DNA polymerases and their role as force generators and molecular motors. Although additional activities are present on many polymerases (e.g., 5'-3' exonuclease [family A], a 3'-5' exonuclease [family A and B],

lyase [family X], or RNAseH (RT family) activities), we will discuss here only advances in our knowledge of the polymerase activity.

II. Biological Diversity of DNA Polymerases

Many different polymerases have been discovered and, based on the primary sequence homologies (Braithwaite and Ito, 1993; Delarue *et al.*, 1990; Ito and Braithwaite, 1991) and crystal structure analyses (Joyce and Steitz, 1994), the different polymerases have been classified into seven different families: A, B, C, D, X, Y, and RT.

A. *Family A*

The family A polymerases can be grouped into replicative and repair enzymes. Enzymes from the bacteriophages T3, T5, and T7 and the eukaryotic mitochondrial DNA polymerase γ are replicative polymerases and interact with other proteins for accurate DNA replication. T7, for example, interacts with bacterial thioredoxin, which acts as a processitivity factor increasing the number of nucleotides added to the DNA chain from 1–15 to several thousand before dissociation of the polymerase (Tabor *et al.*, 1987). Additionally, the T7 polymerase interacts with the T7 DNA primase-helicase and a single-stranded DNA-binding protein (Kornberg and Baker, 1992). Together, this T7 replisome coordinates the synthesis of leading and lagging strand synthesis (Kornberg and Baker, 1992).

The family A repair enzymes include *Escherichia coli* polymerase I (pol I), *Thermus aquaticus* (*Taq*) pol I, and *Bacillus stearothermophilus* pol I. They are involved in nucleotide excision repair and in processing Okazaki fragments that are generated during lagging strand synthesis (Kornberg, 1980). Most pol I enzymes contain a 5'-3' exonuclease activity and a 3'-5' proofreading activity. Only the 5'-3' exonuclease is required for viability because it is necessary for the removal of RNA primers from Okazaki fragments generated during replicative DNA synthesis. The DNA polymerase activity is used to fill in the resulting gap. During repair, pol I enzymes also fill in DNA gaps that result from the removal of a variety of DNA lesions (Kornberg and Baker, 1992).

B. *Family B*

Eukaryotic replicative DNA polymerase α, δ, ϵ, archaebacterial DNA polymerases, viral DNA polymerases, DNA polymerases encoded by mitochondrial plasmids of various fungi and plants, and some bacteriophage

polymerases (T4 and RB69) all belong to family B. Family B polymerases are predominantly involved in DNA replication and carry out processive replication of chromosomal DNA during cell division in eukaryotes. The enzyme participates in leading and lagging strand synthesis and is tethered to the DNA by a processity factor. It is also stimulated by a single stranded DNA-binding protein (Kornberg, 1980). The family B polymerases contain a 3'-5' exonuclease activity that corrects errors during DNA replication. The 3'-5' exonuclease activity of family B polymerases is very strong, being over a 1000 times higher than that of *E. coli* pol I (Capson *et al.*, 1992; Lin *et al.*, 1994).

C. *Family C*

Bacterial family C polymerases are the major chromosomal replicative enzyme (Kornberg and Baker, 1992). Like other replicative polymerases, the holoenzyme interacts with other proteins and forms a large multisubunit complex consisting of at least 10 subunits (Kornberg and Baker, 1992). The α-subunit contains the DNA polymerase activity that is tightly associated with the ϵ-subunit, which contains a 3'-5' exonuclease activity (Kelman and O'Donnell, 1995).

D. *Family D*

Family D polymerases are found in the Euryarchaeota subdomain of Archaea. Although characterization of this family is at an early stage, it is known that the enzyme is heterodimeric (Uemori *et al.*, 1997). The smallest subunit shows low but significant homology to the eukaryotic DNA polymerase δ (Cann *et al.*, 1998), whereas the large subunit is thought to harbor the catalytic region. Characterization of *Pyrococcus furiosus* DNA polymerase II of family D has shown that the enzyme contains both a DNA polymerase activity and a 3'-5' exonuclease activity, and it has been suggested to be a replicative polymerase (Uemori *et al.*, 1997).

E. *Family X*

Known members of the family X polymerases include eukaryotic DNA polymerase β (pol β) (Abbotts *et al.*, 1988), polymerase σ (Burgers *et al.*, 2001), polymerase μ (Dominguez *et al.*, 2000), polymerase λ (Garcia-Diaz *et al.*, 2000), yeast polymerase IV (Prasad *et al.*, 1993), and the African swine fever virus polymerase X (Martins *et al.*, 1994). Pol β is known to be involved in the base excision repair (BER) pathway, which is important for repairing

abasic sites (Matsumoto and Kim, 1995). The enzyme has a modular organization with an 8-kDa amino-terminal domain connected to the carboxy-terminal domain (31 kDa) by a protease-hypersensitive hinge region. The 8-kDa domain contains a 5'-deoxyribose phosphate (dRP) lyase activity that is needed for the process of BER, whereas the large domain contains the DNA polymerase. During BER, the phosphodiester backbone of an abasic site is cleaved 5' to the sugar moiety by an abasic site endonuclease (Matsumoto and Bogenhagen, 1991). DNA pol β cleaves the remaining 5'-deoxyribose phosphate using its dRP lyase activity and fills in the resulting gap using its polymerase activity. The resulting nick is sealed by the action of a DNA ligase (Dianov *et al.*, 2003). The dRP lyase domain also seems to play a role in directing the polymerase to a 5'-phosphate and has single-stranded DNA binding affinity (Kumar *et al.*, 1990). Other members of this family contain additional structural elements, which may be important for function. For example, polymerase λ contains a nuclear localization signal and a breast cancer susceptibility gene (BRCT) domain. The BRCT domain is thought to mediate protein–protein and protein–DNA interactions upon DNA damage (Bork *et al.*, 1997).

F. Family Y

Ultraviolet (UV) irradiation and other mutagenic agents often cause damage to cellular DNA. This can result in physical damage (e.g., base loss creating an abasic site) or modification (e.g., UV crosslinks). Due to the high selectivity and fidelity of replicative DNA polymerases, such damage would stall the replication complex. Recently, a new family of DNA polymerases, family Y, has been identified, the members of which are able to recognize and bypass different classes of lesions on DNA (Friedberg and Gerlach, 1999; Friedberg *et al.*, 2000; Goodman and Tippin, 2000; Johnson *et al.*, 1999; Woodgate, 1999). Family Y polymerases are found in eubacteria, eukaryotes, and archae. The polymerase requires a relatively low specificity to deal with DNA damage. This is reflected in the low fidelity (in the range of 10^{-2}–10^{-4} errors/base replicated) of the polymerase on undamaged DNA and in the lack of an intrinsic 3'-5' proofreading ability (Zhou *et al.*, 2001). Due to their low selectivity, Y polymerases must also function in a distributive manner; they do not remain bound to the DNA during multiple cycles of nucleotide addition, so as not to cause mutagenic incorporation events after lesion bypass is completed. The distributive mode of synthesis should also allow their displacement by the more processive replicative polymerases, thereby reducing their potential mutagenic activity. The family Y polymerases include the DinB (damage-induced) and

UmuC polymerases, which are also known as DNA polymerase IV and V in *E. coli,* respectively, and from eukaryotes, the Rev1 (pol ζ) and Rad30 (pol η) polymerases (Yang, 2003; Zhou *et al.*, 2001).

G. *RT Family*

The reverse transcriptase (RT) family includes RTs from retroviruses as well as the eukaryotic telomerases. During the course of reverse transcription, retroviral RTs interact with a variety of different nucleic acid substrates (RNA/RNA, DNA/RNA, RNA/DNA, DNA/DNA) to convert a single-stranded viral RNA genome into double-stranded proviral DNA (Gotte *et al.*, 1999). Some of the retroviral RTs function as dimers, such as those from the human immunodeficiency virus (HIV) 1 and 2, whereas others, like Moloney murine leukemia virus (MULV) RT, are monomeric. However, both types contain a polymerase domain as well as an RNAseH domain to cleave viral RNA during DNA synthesis. Although they will not be discussed in the context of this review, telomerases also belong to the RT family of polymerases: they use an integral RNA component as a template for synthesis of dGT-rich strands of telomeres (Greider and Blackburn, 1985, 1989).

This review focuses on the polymerases of the A, B, X, Y, and RT families due to the fact that they have been extensively characterized both kinetically and structurally.

III. The Nucleotide Incorporation Pathway

A. *General Theme*

Various studies of DNA polymerases have established a minimal model of nucleotide incorporation for family A (Dahlberg and Benkovic, 1991; Donlin *et al.*, 1991; Eger and Benkovic, 1992; Kuchta *et al.*, 1987, 1988; Patel *et al.*, 1991; Wong *et al.*, 1991), family B (Capson *et al.*, 1992; Lin *et al.*, 1994), family X (Ahn *et al.*, 1997; Kraynov *et al.*, 1997; Werneburg *et al.*, 1996; Zhong *et al.*, 1997), family Y (Fiala and Suo, 2004b; Washington *et al.*, 2001), and RT (Hsieh *et al.*, 1993; Kati *et al.*, 1992; Rittinger *et al.*, 1995; Wöhrl *et al.*, 1999) polymerases. This model is largely common to all polymerases and will be discussed first. Variations on this general theme have been observed and will be discussed next and also in sections below.

The basic model for the nucleotide incorporation by all DNA polymerases is shown in Fig. 1. DNA polymerases catalyze the synthesis of

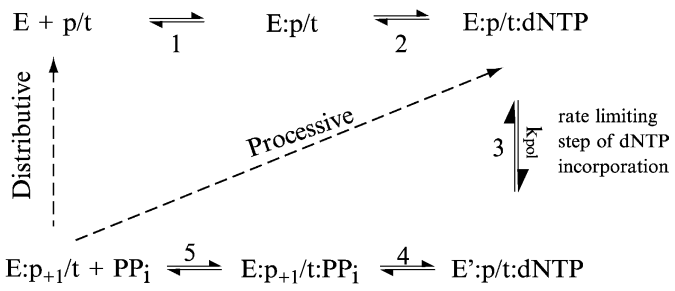

FIG. 1. Kinetic pathway of nucleotide incorporation. The various complexes are indicated as mentioned in the text. ''k_{pol},'' the rate constant of the rate-limiting step, is indicated.

DNA via an ordered mechanism in which the primer template DNA (p/t) binds prior to the dNTP. Polymerization begins with the binding of a p/t to the unliganded enzyme (E) to form the enzyme-p/t complex (E:p/t) (step 1). Nucleotide incorporation into the enzyme-p/t complex is initiated by the binding of a dNTP to the E:p/t complex to form the enzyme-p/t-dNTP complex (E:p/t:dNTP) (step 2). The rate-limiting step of polymerization is the conversion of the E:p/t:dNTP complex to an activated complex, E':p/t:dNTP, which is competent to undergo chemistry (step 3). This rate-limiting step is thought to be caused by a conformational change. The cycle is completed by the nucleophilic attack by the 3'-OH primer terminus on the α-phosphate of the dNTP that results in the formation of a phosphodiester bond (step 4). This is followed by a second conformational change, which allows the release of the pyrophosphate (PPi) product (step 5). The enzyme can then either dissociate from the p/t (distributive synthesis) or translocate the substrate to form a new 3' terminus for a new round of incorporation (processive). If an incorrect nucleotide is incorporated, the new terminus can be partitioned to the 3'-5' exonuclease domain, if present in the polymerase architecture, to be removed. Alternatively, the misincorporated nucleoside can be removed directly by pyrophosphorolysis (the reverse reaction of DNA synthesis), or the polymerase can extend past the incorrect nucleotide, ''sealing'' the misincorporated nucleotide within the elongated strand.

Because step 3 will be discussed in great detail in the sections below, it is appropriate to provide a brief summary of how it was discovered, using the T7 DNA polymerase as an example (Donlin *et al.*, 1991; Patel *et al.*, 1991; Wong *et al.*, 1991). The rate-limiting step was observed when the dependence of the burst amplitude (corresponding to the incorporation of the first nucleotide) on nucleotide concentration was examined. This experiment provided k_{pol} of step 3 (Fig. 1), which was lower than all the other

rates for the preceding chemistry steps. The next question was whether the observed rate was a direct measure of the rate of phosphodiester bond formation. It has been shown that a rate-limiting step involving the making or breaking of a phosphate bond shows a phosphothiate elemental effect. Thus, k_{pol} was measured using both dTTP and dTTP(αS) (the phosphothioate analogue of dTTP) and both values of k_{pol} were compared. These experiments demonstrated a weak elemental effect, indicating that the chemical step is not rate limiting. Thus, the rate-limiting step was ascribed to a conformational change required to form the catalytically competent E':p/t:dNTP complex from the E:p/t:dNTP complex.

Direct observation of the E':p/t:dNTP complex was obtained using pulse-chase experiments. In such experiments, incorporation of labeled nucleotide to an E:p/t complex is either quenched by the addition of HCl or allowed to proceed after the addition of a large excess of ''cold'' unlabeled dNTP (the ''chase'' step) followed by acid quench. In the HCl quench experiments, the acid quenches all the enzyme-bound species. On the other hand, when the reaction is chased with cold dNTP, each of the enzyme-bound species is allowed to partition both in the forward and reverse directions. The amount of partitioning in the forward direction is observed as an excess of labeled product, compared with the acid quench experiment, while the dNTP that partitions in the reverse direction is diluted and remains unobservable. As an excess was observed and because the binding of dNTP to the E:p/t complex is rapid, the observed flux or excess is mainly due to the E':p/t:dNTP complex.

B. Variation on a Theme

Although most polymerases conform to the general kinetic scheme, some polymerases have different mechanisms with regard to p/t binding and selection. Other aspects in the polymerase cycle such as dNTP binding, chemistry, and the conformational change will be discussed in later sections.

Spectroscopic techniques have been applied to monitor nucleic acid binding by both pol β and HIV-1 RT, and the data indicate a more complex binding process than indicated by the general model.

For pol β, it has been shown that binding of gapped DNA is a three-step process (Jezewska *et al.*, 2002). The initial event is thought to involve binding of the nucleic acid by the 8-kDa lyase domain, followed by two docking steps that position the substrate for catalysis (Jezewska *et al.*, 2002). Quantitative studies on pol β have shown that the single-stranded DNA can be bound in two modes that differ in the length of DNA buried by the protein (Jezewska *et al.*, 2001a,b; Rajendran *et al.*, 1998, 2001). This is

thought to be due to the fact that both the lyase domain and the polymerase domain can bind single-stranded DNA. In one binding mode, both the lyase and polymerase domains interact with the DNA. In the second binding mode, interactions with the DNA are mediated exclusively by the lyase domain. Although the lyase domain should not be required for the polymerization mechanism, its removal reduces the efficiency in which polymerization occurs, which may be due to its role in substrate binding (Kumar *et al.*, 1990).

For HIV-1 RT, binding of nucleic acid is a two-step process that is thought to involve the formation of an initial collision complex followed by a conformational change in either the nucleic acid or the protein that ''locks'' the substrate in place (Rittinger *et al.*, 1995; Wöhrl *et al.*, 1999). It has also been shown for HIV-1 RT that binding of the nucleic acid substrate leads to the formation of three types of nucleic acid/protein complexes (Wöhrl *et al.*, 1999). The DNA in one complex is bound in a productive mode and is able to incorporate nucleotides. For the second complex, the enzyme or DNA must undergo a conformational change for nucleotide incorporation to occur. For the third complex, the primer template must first dissociate and reassociate before nucleotide incorporation can occur (Wöhrl *et al.*, 1999). Single-molecule solution-based studies using Fluorescence Resonance Energy Transfer (FRET) confirmed the existence of all three complexes and provided structural information on each (Rothwell *et al.*, 2003). In the first complex (productive complex in product state [PP]), the DNA is indeed bound to the protein in such a way that would allow nucleotide incorporation in the mode observed crystallographically (Jacobo-Molina *et al.*, 1993). In the second complex, the primer terminus now occupies the dNTP-binding pocket (productive complex in educt state [PE]). This would correspond to a state in which dNTP incorporation has occurred, but before translocation of the p/t substrate. The third complex appears to be bound by the epitope recognized by the Fab fragment (PJR unpublished) used to crystallize the binary RT:p/t complex (Jacobo-Molina *et al.*, 1993). The role played by the two latter complexes is not fully understood.

IV. The E State: Basic Architecture of DNA Polymerases

The first DNA polymerase activity was identified in 1956 in *E. coli* (Kornberg *et al.*, 1956; Lehman *et al.*, 1958). The enzyme was subsequently named DNA polymerase I (pol I). *E. coli* pol I is a 109-kDa enzyme that supports a multidomain architecture containing a polymerase activity, a 5'-3' exonuclease activity, and a 3'-5' exonuclease activity. The C-terminal portion of *E. coli* pol I, called the *Klenow fragment,* which lacks the 5'-3'

function (Klenow and Overgaard-Hansen, 1970), was the first DNA polymerase structure to be solved crystallographically (Ollis *et al.*, 1985). The structure of the Klenow fragment has subsequently been solved with DNA bound in the exonuclease site (Beese *et al.*, 1993a; Freemont *et al.*, 1988), and with dNTP and pyrophosphate (Beese *et al.*, 1993b).

From the initial structural studies of the Klenow fragment, the overall shape of the polymerase domain was likened to a right hand, with subdomains referred to as *fingers, palm,* and *thumb* (Fig. 2A), an organization that has been seen for nearly all classes of polymerases solved so far. The polymerase active site, which contains catalytically essential amino acids, is located within the palm subdomain that forms the base of the crevice formed by the fingers and thumb subdomains. The fingers subdomain is important for nucleotide recognition/binding. The thumb subdomain is important for binding the DNA substrate. Subsequent structures of family A polymerases (T7 DNA polymerase, *Taq* DNA polymerase, the Klenow fragment of the *Taq* polymerase [Klentaq1]) and *B. stearothermophilus* DNA polymerase I fragment (BF) show that this topology is conserved (Doublie *et al.*, 1998; Kiefer *et al.*, 1998; Kim *et al.*, 1995; Korolev *et al.*, 1995). For both *Taq* polymerase and the *Bacillus* fragment, the 3'-5' exonuclease is inactive due to both lacking key catalytic residues in this region.

Several structures have been solved for family B enzymes, including those from the bacteriophage RB69 (Franklin *et al.*, 2001; Hogg *et al.*, 2004; Wang *et al.*, 1997b) and from several archaeal organisms (Hashimoto *et al.*, 2001; Hopfner *et al.*, 1999; Rodriguez *et al.*, 2000; Zhao *et al.*, 1999). Like family A polymerases, the general architecture of the polymerase domain is conserved despite very little sequence homology (Fig. 2B). RB69 DNA polymerase is a circular 103-kDa polypeptide with a central cavity. Five separate subdomains surround the cavity. One half of the enzyme constitutes the polymerase domain, containing the fingers, palm, and thumb subdomains named in accordance with the Klenow fragment structure. As with all polymerases, the catalytically important residues are located in the palm subdomain, which can be superimposed with polymerases from different classes. The circle is completed by an N-terminal domain and a 3'-5' exonuclease domain that is homologous to that seen in the Klenow fragment. The N-terminal domain shares homology with RNA-binding domains. Both T4 and RB69 polymerases are able to bind specifically to the ribosome binding sites of their own mRNA to repress their translation; thus, the N-terminal domain is thought to be involved in this process (Pavlov and Karam, 1994; Tuerk *et al.*, 1990; Wang *et al.*, 1997a).

The best characterized family X member is DNA pol β, the smallest eukaryotic polymerase. Although family X polymerases seem to have evolved separately from other classes of DNA polymerases, they share

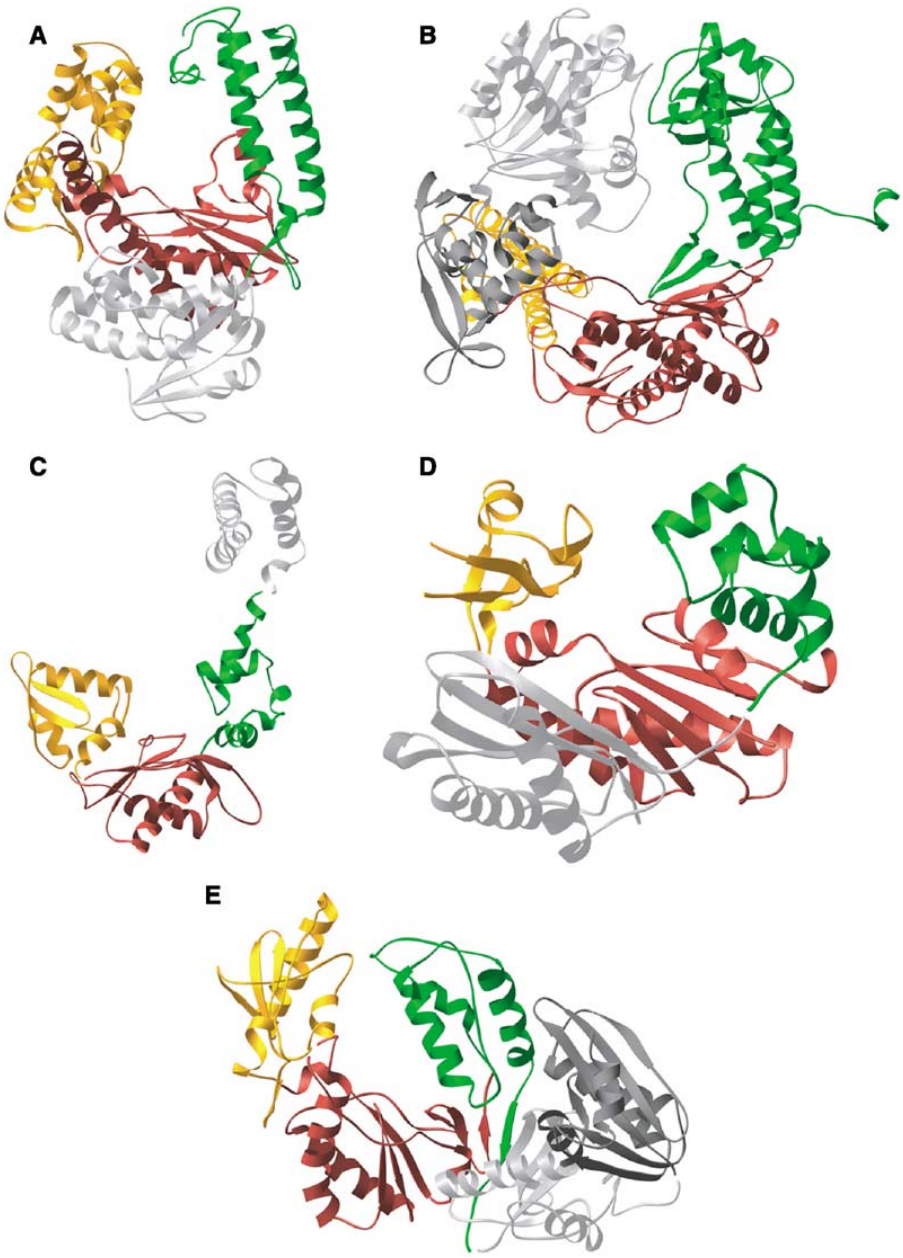

FIG. 2. Structures of family A, B, X, Y, and RT polymerases. The proteins are in ribbon representation. The fingers, palm, and thumb subdomains are color-coded in gold, red, and green, respectively. (A) Structure of apo Klentaq1 (family A). The 3'-5' vestigial exonuclease domain is indicated in silver. (B) Structure of apo RB69 DNA polymerase (family B). The 3'-5' exonuclease domain and the N-terminal domain are indicated in grey and silver, respectively. (C) Structure of apo pol β DNA polymerase (family X). The lyase domain is indicated grey. (D) Structure of the Dpo4 DNA polymerase (family Y). The little finger subdomain is indicated in silver. (E) Structure of the p66 subunit of reverse transcriptase (RT family). The RNAseH and connection subdomains are indicated in grey and silver, respectively.

many common structural features (Fig. 2C). Mammalian pol β is composed of two distinct domains. The C-terminal domain has the overall shape of a polymerase domain and has structures analogous to the fingers, palm, and thumb subdomains, although with little homology (Sawaya *et al.*, 1994). The subdomains were named according to their spatial relationship to conserved features in the palm (Steitz, 1994). The 8-kDa N-terminal domain is tethered to the thumb by a flexible loop. Pol β was the first structure to be solved as an active ternary complex (Pelletier *et al.*, 1994), and the structure has also been solved in the presence of DNA (Pelletier *et al.*, 1994, 1996; Sawaya *et al.*, 1997). The structure of a ternary complex in which the terminal base pair of the nucleic acid substrate contains the DNA lesion 8-oxodeoxyguanine and an incoming nucleotide (Krahn *et al.*, 2003) has also been determined.

Although only identified recently as DNA polymerases, many crystal structures of Y family DNA polymerases have been solved (Ling *et al.*, 2001, 2003, 2004; Nair *et al.*, 2004; Silvian *et al.*, 2001; Trincao *et al.*, 2001; Uljon *et al.*, 2004; Zhou *et al.*, 2001). The structures of the unliganded DinB polymerase from *Sulfolobus solfataricus* (Silvian *et al.*, 2001), of the liganded Dpo4 polymerase from the same organism (Ling *et al.*, 2001), of the unliganded pol η polymerase from *Saccharomyces cerevisiae* (Trincao *et al.*, 2001), and of the liganded human polymerase ι (Nair *et al.*, 2004) reveal the overall architecture of the polymerase domain of family Y polymerases (Fig. 2D). Family Y polymerases share the polymerase domain architecture of family A polymerases. In addition an extra-subdomain is observed, at the C-terminus that is referred to as *little finger, polymerase associated domain* (PAD), or *wrist*. This subdomain is tethered to the thumb subdomain but is physically located next to the fingers subdomain. The binding groove is thus made up of fingers, little finger, palm, and thumb (Ling *et al.*, 2001). The finger and thumb subdomains are both unusually small and lead to a more open and solvent-accessible active site than observed in family A or B polymerases. In contrast to other polymerase families, the structures of some family Y polymerases show that the fingers subdomain appears to be in a closed conformation in the absence of substrate. Also, the enzyme appears to lack any equivalent of the O-helix, which, in family A polymerases, is located in the fingers subdomain and is an important structural feature for nucleotide binding. Instead, it has a β strand and an adjacent extended loop, which is more similar to the arrangement seen in HIV-1 RT (see below).

The structures of MULV (Das and Georgiadis, 2004), HIV-1 (Esnouf *et al.*, 1995; Hsiou *et al.*, 1996; Rodgers *et al.*, 1995), and HIV-2 (Ren *et al.*, 2002) RTs reveal that RT family polymerases share a common architecture of the polymerase domain with family A enzymes. In addition to the

polymerase domain, RTs contain an RNAseH domain, which is used to cleave viral RNA during DNA synthesis. The enzyme also has a connection subdomain, which connects the RNAseH domain to the polymerase domain. Both HIV enzymes function as heterodimers (Divita *et al.*, 1995a,b) composed of two related chains. For example, HIV-1 RT consists of a 66-kDa subunit (p66) and a 51-kDa subunit (p51) derived from p66 by proteolytic cleavage. MULV RT is monomeric (Das and Georgiadis, 2004; Roth *et al.*, 1985).

HIV-1 RT is the best structurally characterized of this family (Fig. 2E). High-resolution structures are available of HIV-1 RT in unliganded form (Esnouf *et al.*, 1995; Hsiou *et al.*, 1996; Rodgers *et al.*, 1995), bound to non-nucleoside RT inhibitors (NNRTIs) (Ding *et al.*, 1995a,b; Kohlstaedt *et al.*, 1992; Pata *et al.*, 2004; Ren *et al.*, 1995, 1998, 2004; Smerdon *et al.*, 1994), in complex with nucleic acid substrates (Ding *et al.*, 1998; Huang *et al.*, 1998; Jacobo-Molina *et al.*, 1993; Jaeger *et al.*, 1998; Sarafianos *et al.*, 2001, 2002), or in a ternary complex with p/t DNA and nucleotide (Huang *et al.*, 1998). Both subunits of this heterodimeric enzyme, p66 and p51, contain four subdomains (fingers, palm, thumb, connection) (Kohlstaedt *et al.*, 1992). In addition, the p66 subunit contains the RNAseH domain. Although the structure of the subdomains within p66 and p51 are similar, the relative arrangement of the subdomains within the subunits is different. The p51 subunit, despite containing the components of a polymerase active site, has no catalytic activity and is thought to stabilize the dimer.

Perhaps the most obvious difference in the HIV-1 RT, compared with family A, B, and X polymerases, is in the fingers subdomain. Family A, family B, and pol β, all have an α-helical region that forms part of the dNTP-binding site and is important for nucleotide selection. For HIV-1 RT, a region of antiparallel β-ribbon (β3–β4) fulfills this role. The apo form of HIV-1 RT was solved crystallographically in both ''open'' and ''closed'' forms, corresponding to a different position of the thumb subdomain, either closer to the opposite fingers (closed) or farther away (open). Subsequently, EPR measurements showed the enzyme to be predominantly in a closed conformation (Kensch *et al.*, 2000). Molecular dynamics simulations also suggest that the closed conformation is also favored for the unliganded enzyme (Madrid *et al.*, 1999). This closed form should not be confused with the closed structure of the ternary complex bound to DNA and nucleotide (see Section VII). However, the thumb subdomain can also adopt an even more open form: NNRTI binding induces an additional hinge movement of the p66 thumb subdomain near the thumb's knuckle, causing the p66 thumb subdomain to adopt a configuration that is even more extended than in the open apo and DNA-bound RT structures (see below) (Hsiou *et al.*, 1996; Smerdon *et al.*, 1994).

V. Primer/Template DNA Binding and Recognition

The initial event in the nucleotide incorporation cycle is binding of the double-stranded p/t DNA to the polymerase to form the E:p/t complex (Step 1; Fig. 1). Many structures now exist, in which DNA is bound at the polymerase active site.

The structure of the E:p/t complex for the Klenow fragment of the *Taq* polymerase, Klentaq1, shows the overall binding mode of DNA for family A polymerases (Li *et al.*, 1998b; Fig. 3A). When compared with the apo form of the enzyme, this structure shows that DNA-binding results in structural changes mostly localized in the thumb subdomain (Fig. 3B). The movement corresponds to an initial opening of the thumb followed by a rotation in the opposite direction that brings residues in the tip of the thumb closer to the DNA (Li *et al.*, 1998b). The movements in the thumb are mostly localized to a helix-loop-helix motif at the tip of the thumb, which, for structures not containing bound DNA, is disordered, suggesting a high degree of flexibility. The net result of the thumb movement is to form a cylinder that completely surrounds the DNA. The wrapping of the domain around the DNA may hold the DNA during processive polymerization. Residues within the palm subdomain interact with the template strand along the minor groove. The 3' terminus of the primer is held near the polymerase active site in the palm subdomain. Neither the duplex DNA nor the single-stranded template passes through the crevice between the fingers and the thumb subdomains; rather, the single-stranded part of the DNA template is flipped out of stacking arrangement with the duplex by a sharp angle in the template sugar-phosphate backbone, which positions the single-stranded template on the same side of the crevice as the duplex DNA (Fig. 3C). A Tyr (671 for Klentaq, 714 for BF, 766 for Klenow) at the C-terminus of the O-helix is inserted into the stacking arrangement of the template bases, lying directly on top of the first base pair of the duplex part of the DNA (Fig. 3C). This residue may act as a positioning device for the p/t such that the first base pair of the duplex can register itself against the active site. Interestingly, in the complex of Klentaq1 bound to a nucleotide (see Section VI), although the conformation of the fingers subdomain is the same (i.e., open), Tyr671 is not seen, suggesting a high degree of flexibility in the absence of DNA (Li *et al.*, 1998a). The bound DNA is mostly in the B-form, except for the last three bases closest to the polymerase active site, which are in the A-form. The DNA is distorted to assume an S-shape: the first bend is caused by interactions within the palm subdomain and the second bend is caused by interactions with the thumb. A similar arrangement is seen for other family A polymerases with bound DNA (Doublie *et al.*, 1998; Eom *et al.*, 1996; Kiefer *et al.*, 1998).

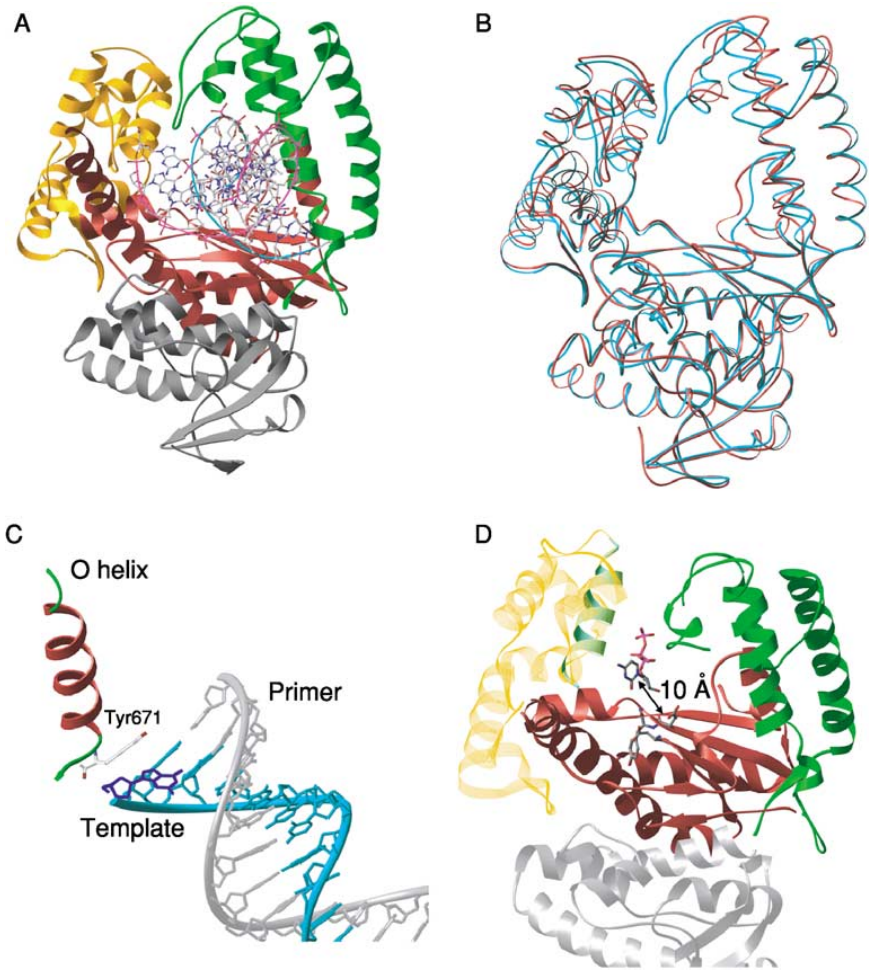

FIG. 3. Structure of the p/t DNA bound Klentaq1. (A) Overall structure of the Klentaq1 bound to a p/t DNA. The protein is in ribbon representation, whereas the p/t DNA is in both ribbon and ball-and-stick representation. The fingers, palm, and thumb subdomains are color-coded as in Fig. 2, whereas the vestigial 3'-5' exonuclease is colored grey. The primer strand ribbon is in cyan, and the template strand ribbon is in magenta. (B) Superimposition of the apo (red) and p/t-bound (cyan) Klentaq1. Only the protein is shown and is in ribbon representation. The orientation is the same as in Fig. 3A. The DNA-bound structure differs from that of the apo form by a conformational change in the thumb subdomain. (C) Location of Tyr 671 and the templating base in the E:p/t complex. The O-helix is labeled and is shown in red ribbon representation. The primer and template strands are in both ribbon and ball-and-stick representation. The primer and template strands are in silver and cyan, respectively. The first single-stranded template base (the templating base) is in deep blue. Tyr 671 is seen stacked on top of the template base of the first duplex base pair, and the templating base is flipped out. (D) Model of a dNTP bound to the O-helix of Klentaq1 in the E:dNTP complex and its position relative to active site. The subdomains are color-coded as in Fig. 3A. The various subdomains are in ribbon representation with lined instead of filled-in ribbons for the fingers subdomain. This allows the visualization the O-helix in pale green in the fingers domain. The distance between the base of the dNTP and the active site residues is indicated.

Recently, a binary complex of RB69 DNA polymerase (family B) was solved bound to a furan containing p/t DNA (Hogg *et al.*, 2004). Although the bound DNA represents a state in which the DNA has not translocated after incorporation, it does give an overall idea of how the DNA is bound by family B polymerases. Like the apo form of the enzyme, the fingers subdomain is in an upright conformation (Wang *et al.*, 1997b). In contrast to family A polymerases, the DNA is bound in the B-form throughout. However, like family A polymerase, the single-stranded region of the template is flipped out of the stacking arrangement with the duplex part of the DNA.

Binding of a p/t DNA with a four-base template overhang to pol β (family X) results in an inward movement of the 8-kDa N-terminal domain to form a more compact structure. Although the 8-kDa domain does not interact with the DNA, it approaches close to where a longer template overhang would presumably locate (Pelletier *et al.*, 1994). The pol β:DNA complex structure has also been determined with a gapped DNA substrate (Sawaya *et al.*, 1997). In this form, the DNA is held and the gap opened by the concerted action of the 8-kDa lyase domain, which grips the DNA downstream of the gap and interacts with the 5' phosphate and the polymerase domain that holds the substrate upstream of the gap. This introduces a 90-degree kink into the DNA, which has B-form characteristics on both sides of the kink (Pelletier *et al.*, 1996; Sawaya *et al.*, 1997). Compared with the recessed p/t substrate-bound model of pol β, the 8-kDa domain is in an even more compact closed form and interacts with the fingers subdomain.

From the structure of the ternary E':p/t:ddNTP complex for the Dpo4 polymerase (family Y; see also Section VII), it can be seen that the DNA bound by the polymerase domain of family Y polymerases is in the B-form throughout (Ling *et al.*, 2001). The DNA bound to family Y polymerases is more solvent exposed than DNA bound to family A or B polymerases. The Dpo4 polymerase makes relatively few contacts with the DNA outside the active site, and the bound DNA buries less than 600 Å of the molecular surface of the catalytic core (fingers, palm, and thumb) compared with 1000 Å in family A and B polymerases (Ling *et al.*, 2001). However, the little finger seems to increase the overall interaction of the DNA with the protein. It contains a four-stranded β-sheet and two parallel α-helices. The β-sheet interacts with the DNA to increase the contact surface area. The thumb and the little finger grip the nucleic acid across the minor groove. Family Y polymerases lack an equivalent to the Tyr residue of family A polymerases (Tyr 671 of Klentaq1 for example), which is seen to insert into the stacking arrangement of the template bases, lying directly on top of the duplex part of the DNA (Ling *et al.*, 2001). Interestingly, mutations of this tyrosine residue to smaller side

chains in family A polymerases result in a ''family Y–like'' mutator phenotype (Carroll *et al.*, 1991).

For the DNA-bound forms of HIV-1 RT (RT family), it can be seen that the thumb is rotated outward when compared with the unliganded structure (Ding *et al.*, 1998; Jacobo-Molina *et al.*, 1993). In the RT:p/t complex, the p66 thumb subdomain adopts an upright position, as opposed to the ''closed'' unliganded structure (Hsiou *et al.*, 1996; Rodgers *et al.*, 1995). This movement results in an opening of the structure, generating a large DNA-binding cleft that extends over 60 Å from the N-terminus of the polymerase domain to the C-terminal RNAseH domain. The position of the other subdomains remains largely unchanged. For HIV-1 RT, the first five base pairs of the p/t substrate are in A-form, followed by a four–base pair region that introduces a sharp kink of about 40–45 degrees that then leads to a B-form DNA. This large region of A-form DNA may be important in binding RNA/RNA and RNA/DNA duplexes, which are expected to adopt an A-form (Kornberg and Baker, 1992). The 5'-template (resolved for three bases in the ternary E':p/t:ddNTP complex structure by Huang *et al.* (1998; see Section VII) bends away from the duplex by a sharp angle and packs against residues on the surface of the fingers subdomain.

VI. Formation of the E:p/t:dNTP Complex

Nucleotide incorporation into the enzyme-p/t complex is initiated by the binding of a dNTP to the E:p/t complex to form the E:p/t:dNTP complex (Step 2; Fig. 1).

Step 2 in the nucleotide incorporation cycle is an important step at which the enzyme is able to discriminate between correct versus incorrect nucleotides. However, the efficiency with which different polymerases bind correct or incorrect dNTPs at this step varies greatly. The replicative polymerases discriminate with high efficiency against incorrect nucleotides during Step 2. The K_D differences between correct and incorrect ($K_{D(dNTPcorrect)}/K_{D(dNTPincorrect)}$) range from 390-fold for T7 DNA polymerase (family A) to 263-fold for T4 DNA polymerase (family B) and 250-fold for HIV-1 RT (Gillin and Nossal, 1976; Kati *et al.*, 1992; Topal *et al.*, 1980; Wong *et al.*, 1991). For the repair enzymes, the differences between correct and incorrect nucleotide binding are much smaller. The Klenow fragment (family A) only selects against incorrect nucleotide incorporation on average by a factor of 3.4, yeast polymerase η (family Y) by a factor of 4, and polymerase β (family X) by a factor of 20 (Ahn *et al.*, 1997; Kuchta *et al.*, 1987, 1988; Washington *et al.*, 2001; Werneburg *et al.*, 1996). This suggests that initial dNTP recognition at Step 2 is defined by function (replicative vs. repair) rather than family.

Although the E:p/t:dNTP complex has not been captured structurally with a native p/t DNA-bound substrate, both the Klenow fragment and Klentaq1 have been crystallized in the presence of all four nucleotides (Beese *et al.*, 1993b; Li *et al.*, 1998a). In this form, all four nucleotides are bound by the N-terminal end of the O-helix in the fingers subdomain. The triphosphate group of the dNTP is within the range of electrostatic interactions with the positively charged side chains of Arg659 (754 in *E. coli* pol I), Lys 633 (758 in *E. coli* pol I), and Arg587 (682 in *E. coli* pol I), with the triphosphate moiety running parallel to the O-helix (Fig. 3D). The base of each dNTP points toward the DNA-binding cleft, although the electron density indicates in each case that there is disorder. The position of the triphosphate moiety of the nucleotide is nearly identical for all bound nucleotides, suggesting that the initial recognition of the incoming nucleotide is through the triphosphate. Characterization of mutations of O-helix residues Arg754 and Lys758 in *E. coli* pol I shows that they both greatly affect the $K_{M(dNTP)}$ and $K_{M(PPi)}$ and have little or no effect on DNA binding (Astatke *et al.*, 1995; Suzuki *et al.*, 1996). Lys758 of *E. coli* pol I was also identified as the site of labeling with pyridoxal 5'-phosphate (PLP), a compound that binds specifically to triphosphate-binding sites (Basu and Modak, 1987). When bound to the O-helix, the nucleotide is far away (10–15 Å) from the active site located in the palm (Fig. 3D) and, thus, a large conformational change affecting the fingers subdomain must be invoked to ''deliver'' the nucleotide to the active site of the enzyme (see next section).

Recently, an E:p/t:dNTP complex was captured for the T7 (family A) DNA polymerase, a high-fidelity DNA polymerase, in the presence of a p/t DNA containing a *cis-syn* thymine dimer (Li *et al.*, 2004). Although this type of lesion may impede the closing of the fingers subdomain in the presence of dNTP, it does add evidence that binding within the O-helix is the initial event of the nucleotide incorporation cycle for family A polymerases. However, this triphosphate-mediated binding would not provide the high-level discrimination between correct and incorrect nucleotides displayed by T7 DNA polymerase. It is therefore unlikely that this complex represents the E:p/t:dNTP complex observed kinetically. However, it cannot be ruled out that, in the presence of a ''conventional'' p/t DNA substrate, additional constraints are imposed on dNTP binding.

Recent kinetic work on RB69 polymerase (family B) and structural comparison between the RB69 polymerase and other polymerase families led to the postulation of a different initial binding event for dNTP (Yang *et al.*, 2002a). The crystal structure of the closed ternary E':p/t:ddNTP complex of the RB69 polymerase (see Section VII) shows interactions between the fingers subdomain and the ddNTP's triphosphate moiety

similar to those observed in family A polymerases (Doublie *et al.*, 1998; Franklin *et al.*, 2001; Li *et al.*, 1998b). However, it was suggested that, due to the greater discrimination at Step 2 between correct and incorrect nucleotides displayed by family B members compared with family A repair enzymes, the nucleotide would diffuse directly into the polymerase active site (Yang *et al.*, 2002a). This would allow the RB69 polymerase to probe correct versus incorrect base pairing directly. The difference in affinity between correct and incorrect nucleotides would result in only correct nucleotides remaining bound long enough for the formation of the closed ternary E':p/t:dNTP complex, a conformation that seems to be required for catalysis (see next section).

Mutational work on human DNA polymerase α also supports a different initial recognition of nucleotide by family B members. Mutations within the conserved motif II, which contains one of the catalytically important aspartates, reduce the affinity of correct nucleotides (Dong *et al.*, 1993), suggesting that residues in motif II form both the dNTP-binding region and the catalytic site. Based on these results, one could argue that the dNTP-binding site is located in close proximity to the active site, possibly coinciding. Thus, DNA-binding would position the templating base (the first base of the template's single-stranded overhang) within the dNTP-binding site, providing a powerful readout of correct versus incorrect nucleotide binding through W-C pairing. Consistent with this hypothesis, while wild-type human DNA polymerase α (like other family B polymerases) strongly discriminates at the dNTP-ground state binding stage with $K_{MdTTP(correct)}/K_{MdATP(incorrect)}$ being over 2000, mutations of Tyr865 within motif II (a mutation shown to reduce dNTP-binding but not DNA-binding) to Ser reduces discrimination by a 20-fold, whereas mutation to Phe has little effect on activity and discrimination (Dong *et al.*, 1993).

VII. Conformational Transition to a Catalytically Active Ternary Complex: The E':p/t:dNTP Complex

The rate-limiting step in the kinetic pathway of nucleotide incorporation is the conversion of the E:p/t:dNTP complex to the activated complex, E':p/t:dNTP (Step 3 in Fig. 1). This step is crucial in many respects. First, it is essential for the phosphoryl transfer reaction to occur. During the E:p/t:dNTP to E':p/t:dNTP transition, all the components of the active site are assembled and organized in a topological and geometrical arrangement that allows the enzyme to proceed with the chemical step (Step 4). Second, Step 3 plays a major role in the mechanism of discrimination between correct versus incorrect nucleotides. Interpretation of the kinetic measurements has led to the hypothesis that the E:p/t:dNTP

to E':p/t:dNTP rate-limiting step is caused by a slow conformational change in the binding partners. In this section, we will first describe the various attempts that structural biologists have made to elucidate the molecular basis of this kinetically defined conformational change. We will next describe the mutational, kinetic, and computational work that has challenged the conclusions of the structural biology work. Finally, in a third section, we will discuss the mechanism of nucleotide discrimination at Step 3.

A. Structures of E':p/t:ddNTP Complexes

The E':p/t:dNTP complex is a transient complex and thus cannot be captured crystallographically as is. However, by using dideoxyribonucleoside triphosphates (ddNTP) in a reaction that involves a E:p/t binary complex where the primer is terminated by a ddNMP, Kraut and colleagues have shown that a ternary complex of pol β can be obtained where the catalytic residues, the Mg ions, the p/t DNA, and the ddNTP appear to be ''trapped'' in a chemistry-competent state (Pelletier *et al.*, 1994). Thus, in the presence of a terminated primer, the incoming ddNTP appears to be able to trigger the conformational changes required to form a catalytically competent complex. However, due to the fact that ddNTP lack the 3' OH group, chemistry cannot occur. The difference in the structures on going from the binary E:p/t complex to the ternary E':p/t:ddNTP complex shows large conformational changes that are described below.

Formation of the ddNTP-trapped ternary complex (E':p/t:ddNTP) of Klentaq1 (family A) results in a large reorientation of the fingers subdomain (Fig. 4; Li *et al.*, 1998b). The effect of the conformational transition affecting the fingers subdomain is to position the O-helix in two different conformations (Fig. 4B). In the first conformation (termed *open*), the O-helix is in the configuration of the apo and DNA-bound enzyme. Tyr671 is inserted into the stacking arrangement of the template base and lies on top of the first base pair of the duplex DNA (Fig. 3C). In the second orientation (termed *closed*), seen in the ddNTP-trapped ternary complex, the O-helix has moved inward by 46 degrees and is now much closer to the active site formed by the three carboxylates located in the palm domain. During this transition, the side chain of Tyr671 is released from the stacking arrangement with the template base (Fig. 4C). This allows the first single-stranded DNA base of the template (the templating base) to position itself in front of the incoming nucleotide (Fig. 4C). The ddNTP is bound to the O-helix and is stacked onto the 3' base of the primer strand. Two metal ions (Mg^{2+}) are bound to the catalytic aspartate residues (Asp 610 and Asp 785) and to the nucleotide (see mechanism in

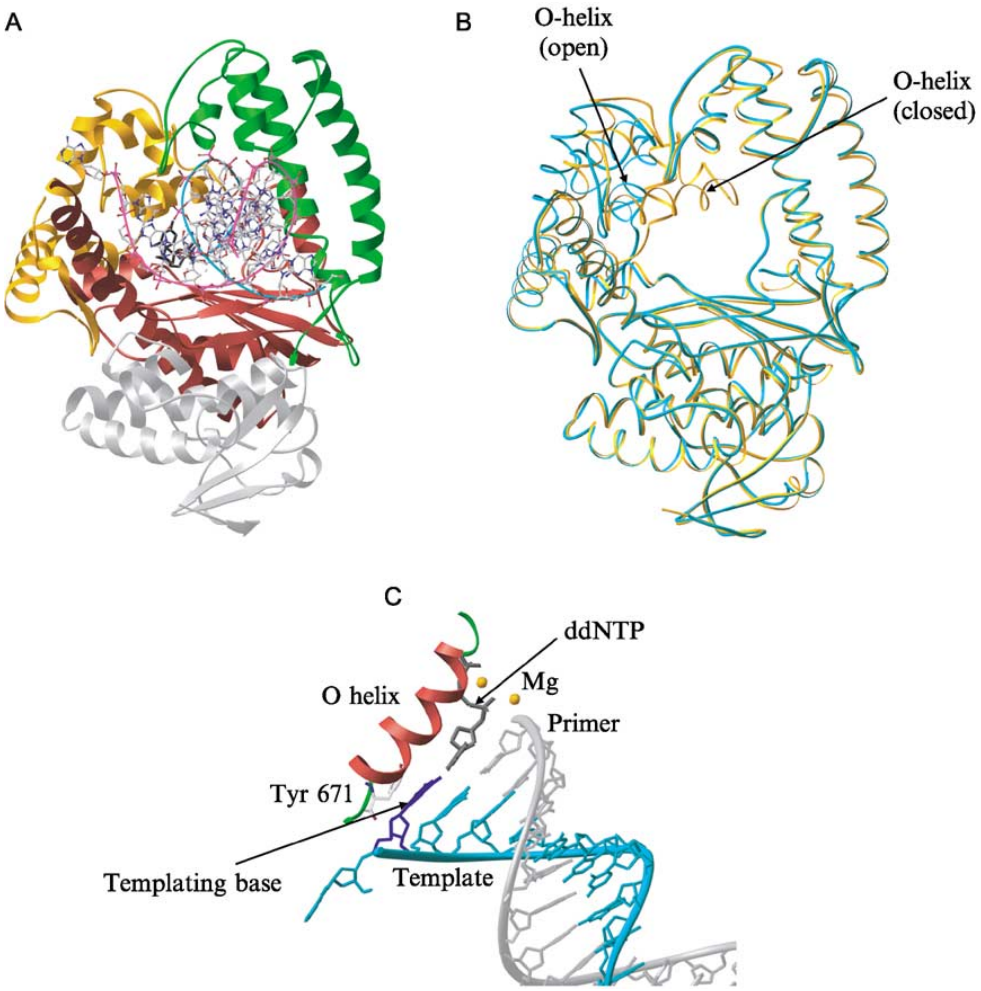

FIG. 4. The open-to-closed conformational transition affecting the fingers subdomain. (A) Structure of the Klentaq1 E':p/t:ddNTP complex. See legend of Fig. 3A for key to color coding. The ddNTP is indicated in black but is hardly visible in this orientation. (B) Superimposition of the E:p/t (cyan) and E':p/t:ddNTP (gold) complexes. Only the protein is shown in ribbon representation. The orientation is the same as in (A). The O-helix is indicated in both conformations. The ternary complex differs from the binary complex by a large conformational change affecting the O-helix. (C) Location of Tyr 671 and the templating base in the E':p/t:ddNTP complex. See legend of Fig. 3A for key to color coding. The incoming ddNTP nucleotide is colored black and is located in front of the templating base in deep blue. The Mg^{2+} ions are indicated in gold balls.

Section VIII). In this closed form of the enzyme, the complex appears to be poised for chemistry. One of the striking features of the ternary complex described above is the close fit of the protein around the nascent base pair in the closed ternary complex (Li and Waksman, 2001a; Li *et al.*, 1998b).

Such a snug fit of the protein and DNA around the nascent base pair provides a most efficient steric readout for appropriate base pairing and is thought to play a fundamental role in the mechanism of discrimination between correct versus incorrect nucleotide (see below).

In the active ternary complex of the RB69 polymerase, the fingers subdomain is in a closed conformation as seen in family A polymerases (Franklin *et al.*, 2001). The rotation of the fingers subdomain inward brings conserved residues of the finger, which contact the triphosphate moiety, close to the active site. One interesting consequence of the fingers subdomain movement in RB69 polymerase is that the finger domain now makes direct contact with the exonuclease site (Franklin *et al.*, 2001). This may be important in transmitting structural changes caused by misincorporation to the exonuclease site.

Several structures of ternary E':p/t:ddNTP complexes of a family Y polymerase, Dpo4, have also been determined (Ling *et al.*, 2001, 2004). Two forms of the ternary E':p/t:ddNTP complex have been solved, one in which the correct nucleotide is present for incorporation and the other in which an incorrect nucleotide is provided (Ling *et al.*, 2001). For the correctly base paired E':p/t:ddNTP complex, the newly formed base pair is less protected than in the replicative polymerases due to a more solvent exposed active site. In the second form, the first templating base is a G followed by a C, and Ling *et al.* supplied ddGTP. A G:G mismatch has been shown to be disfavored by this enzyme, with a mismatch frequency of 3.5×10^{-4} (Boudsocq *et al.*, 2001). Interestingly, the enzyme skips the G base by translocating the p/t substrate so that the ddGTP can base pair with the C. This mechanism of incorporation may be important in translocating through certain lesions, such as *cys-syn* cyclobutane pyrimidine dimers (CPD). From the structures of the ternary complexes, a mechanism by which the enzyme can bypass *cys-syn* CPD was suggested (Ling *et al.*, 2001) and was later refined by the determination of two structures of Dpo4 in a complex with a p/t DNA carrying a CPD and ddATP (Ling *et al.*, 2004). In these latter structures, the 3' thymine of the CPD forms a W-C base pair with the incoming ddATP, but the 5' thymine forms a Hoogsteen base pair with the ddATP in *syn* conformation. Dpo4 retains a similar tertiary structure, but each unusual DNA structure is individually fitted into the active site for catalysis.

A rate-limiting step corresponding to a conformational change has been observed in family Y polymerases (Fiala and Suo, 2004a,b; Washington *et al.*, 2001). However, it has been difficult to ascertain the nature of the conformational change for family Y members due to the fact that no complete set of structures (e.g., E, E:p/t, E':p/t:ddNTP) is available for a single polymerase from this family. However, it has been suggested, based

on superimposition of the structure of yeast pol η apo form (Trincao *et al.*, 2001) and those of the Dpo4 ternary complexes (Ling *et al.*, 2001, 2004), that a 48-degree inward rotation of the fingers and little finger subdomains occurs (Fiala and Suo, 2004a). However, in the case of Dbh, the apo form of the enzyme (Silvian *et al.*, 2001) appears to be in a closed conformation, and superimposition of the structure with the ternary complexes of Dpo4 (Ling *et al.*, 2001) shows no obvious conformational change (Fiala and Suo, 2004a). Therefore, the nature of the conformational change detected by pre–steady state kinetic analysis (Fiala and Suo, 2004a,b; Washington *et al.*, 2001) remains unclear for Y family DNA polymerases.

For HIV-1 RT, binding of the incoming nucleotide substrate, in the presence of bound p/t, also results in a structural rearrangement in the fingers subdomain (Huang *et al.*, 1998). This structural rearrangement results in a 20-degree inward bending of the outer part of the fingers subdomain towards the palm subdomain. It is not yet clear whether the dNTP is ''delivered'' to the active site by initial binding of the triphosphate moiety to the fingers subdomain, as would seem to be the case for family A polymerases. Nevertheless, like Klentaq1, the closure of the fingers subdomain results in the formation of a pocket that accommodates the nascent base pair. Residues in the fingers subdomain coordinate the triphosphate moiety of the incoming nucleotide. The 3'-OH of the incoming nucleotide projects into a pocket referred to as the 3'-OH pocket. This pocket is important and has been exploited in the design of nucleoside RT inhibitors (NRTIs) used in retroviral therapy (for review, see Sluis-Cremer *et al.*, 2000).

The pol β:p/t:ddCTP structure shows that, in the absence of a downstream DNA fragment, the lyase domain does not interact with the DNA and is positioned some distance from the active site (Pelletier *et al.*, 1994). However, in a structure solved with gapped DNA, the lyase domain binds to the 5'-phosphate in the DNA gap and interacts with its own carboxy-terminus in the thumb (Sawaya *et al.*, 1997). In common with all polymerases, the fingers subdomain closes down around the correct nucleotide and its complementary template base. This motion corresponds to a 30-degree rotation of α-helix N (the dNTP-binding site) around α-helix M and thus brings helix N and its bound nucleotide into position to probe correct W-C base pairing.

B. Molecular Basis for the Rate-Limiting Step

With the crystallographic data of different states in the nucleotide incorporation cycle now available, it is tempting to believe that the conformational change identified by kinetic experiments at step 3 could be

due to the closing of the fingers subdomain observed structurally on binding of the ddNTP to the E:p/t complex. However, recent mutational, kinetic, and computational studies have challenged these conclusions.

Mutational work on pol β led to the suggestion that the open-to-closed transition affecting the fingers subdomain (and in particular, helix N) observed crystallographically is not the rate-limiting conformational change (Pelletier *et al.*, 1994). Asp 276 in α-helix N makes contact with the incoming nucleotide only in the closed conformation of pol β. Remarkably, a mutation of this residue to Val results in an increase in free energy in dNTP ground-state binding (Vande Berg *et al.*, 2001). This result strongly suggests that the rate-limiting conformational change is not the open-to-closed structural transition, but instead is triggered in the closed polymerase conformation. Vande Berg *et al.* suggested a three-step binding model in which the dNTP initially binds in a nonspecific manner through either the triphosphate or the sugar moiety. This step is associated with weak binding so as to facilitate rapid sampling of the nucleotide pools and is not kinetically resolvable. They further suggested that this rapid-sampling step is associated with the open-to-closed transition seen crystallographically when going from the binary E:p/t complex to the ternary E':p/t:ddNTP complex. During the second step, bases are selected due to base pairing and steric complementarity at the polymerase active site. In the presence of a correct nucleotide, steric complementarity in the closed form of the ternary complex triggers the kinetically defined rate-limiting conformational change, which results in the final alignment of all components participating in the reaction (Vande Berg *et al.*, 2001). Similar conclusions were drawn from inspection of the rate-limiting kinetics of wild-type pol β and a pol β variant mutated at Tyr265, a residue that does not make any contact with the DNA or the dNTP (details on the wild-type enzyme are provided in Section VII.C; Shah *et al.*, 2003; Zhong *et al.*, 1997). This mechanism would also apply to family A polymerases, in which a nucleotide is bound in the O-helix in the open conformation. A fast conformational change of the O-helix would allow the bound nucleotide to be delivered to the active site. At this stage, correct base-pairing would trigger a conformational change, whereas incorrect base-pairing would result in the nucleotide leaving the active site (Vande Berg *et al.*, 2001).

Conformational transitions in the Klenow fragment have been examined by stopped-flow fluorescence using DNA substrates containing the fluorescent reporter 2-aminopurine (2-AP) on the template strand, either at the templating position opposite the incoming nucleotide or 5' to the templating base (Purohit *et al.*, 2003). It was shown that the 2-AP reporter at the templating position undergoes a sizable and very rapid decrease in fluorescence associated with dNTP binding. Comparison of

the structures of the E:p/t and E':p/t:ddNTP complexes in Klentaq1 shows that the templating base must undergo a very large conformational change to position itself in the stacking arrangement with the duplex part of the p/t DNA (Figs. 3C and 4C). However, in the open form, this position is occupied by Tyr 671 and thus Tyr 671 must move. This is achieved by the rotation of the O-helix during the open-to-closed transition, which takes Tyr 671 with it, thereby liberating the space into which the templating base can come (Figs. 3C and 4C). As the motion of the templating base is fast, the open-to-closed conformational transition affecting the O-helix must be at least as fast.

These data appear to indicate that the open-to-closed transition affecting the fingers subdomain is very fast and not rate limiting. Note that this evidence is all indirect and that the rate of the open-to-closed conformational transition has not been measured. However, all data are indicative of a fast motion. This is counterintuitive because the fingers subdomain is relatively big and one may have difficulties envisaging that such a large domain motion could be fast. However, direct evidence for a rapid motion of the fingers subdomain has been provided. To probe the microenvironment and dynamics of α-helix N in the polymerase domain of pol β, the single native tryptophan (Trp 325) was removed, and a tryptophan was strategically placed near the end of α-helix N (Kim *et al.*, 2003). Influences of substrates on the fluorescence anisotropy decay of this single tryptophan form of pol β were determined. The results revealed that the segmental motion of α-helix N was rapid (~1 nsec) and far more rapid than the step that limits chemistry. Binding of a correct dNTP significantly limited the angular range of the nanosecond motion within α-helix N, whereas binding of a p/t or gapped DNAs had minor effects. These results again argue that the rate-limiting step is not the conformational transition observed crystallographically (Pelletier *et al.*, 1994).

Although the experiments described above are instructive, they still leave the question open as to the nature of the rate-limiting conformational change. This process was investigated in more detail using computer simulations (Yang *et al.*, 2002b). Again, the suggestion was that the closing of α-helix N was rapid and that the rate-limiting conformational change may correspond to more subtle movements of side-chains within the active site. Further simulations of pol β substrate-induced dynamics showed a role for Mg^{2+} in the formation of the E':p/t:dNTP complex (Yang *et al.*, 2004). The results showed that the closing of the fingers subdomain is favored in the presence of Mg^{2+}, and removal of Mg^{2+} favors the reopening of the subdomain. The sequence of events proposed to occur during the nucleotide incorporation cycle is as follows: (1) binding of the dNTP:Mg^{2+} to the open pol β:p/t complex; (2) binding of the catalytic Mg^{2+};

(3) relatively fast conformational transition of the fingers subdomain from an open to closed state; (4) slow, possibly rate-limiting assembly of the key amino acids residues, template bases, Mg^{2+} ions, and the primer 3'-OH group; (5) slow and possibly rate-limiting chemical step of the nucleotidyl transfer reaction; (6) release of the catalytic Mg^{2+}; (7) relatively fast conformational transition from the closed-to-open complex state again involving subtle residue motions; (8) release of the product PPi/Mg^{2+} (Yang *et al.*, 2004).

Computer simulations must be met with a degree of skepticism. However, these will no doubt suggest experiments aimed at confirming or perhaps disproving their conclusions.

C. Discrimination Between Correct Versus Incorrect Nucleotide

How do the processes described above contribute to fidelity? Steps 2 and 3 of the nucleotide incorporation cycle are the most important steps in the mechanism of nucleotide discrimination. Discrimination at Step 2 has been discussed in Section VI. Here we discuss the role of Step 3 in that process.

Much of the discrimination against the incorrect nucleotide occurs at Step 3, although here again the degree to which the enzyme is able to discriminate against incorrect nucleotide incorporation varies, as does the extent to which the rate-limiting step contributes to it.

Quench flow studies on both T7 and Klenow fragment (family A) show that both strongly discourage nucleotide misincorporation, as measured by the ratio of $k_{pol(correct)}/k_{pol(incorrect)}$, by slowing Step 3 by a factor of 2000 and 5000, respectively (Kuchta *et al.*, 1987, 1988; Patel *et al.*, 1991; Wong *et al.*, 1991). Due to observed elemental effects, it was thought that for T7 DNA polymerase, the rate-limiting step was due to a conformational change irrespective of whether correct or incorrect nucleotides are incorporated (Patel *et al.*, 1991). For the Klenow fragment, however, nucleotide incorporation of the correct nucleotide is limited by the conformational change, while, in the case of misincorporation, Step 4 (chemistry) becomes rate-limiting (Patel *et al.*, 1991). Nucleotide incorporation into a (2-AP)-containing p/t DNA substrate by the Klenow fragment indicated that a conformational change occurs during misincorporation, but the chemical step determines the slowest rate (Frey *et al.*, 1995).

HIV-1 RT has an extremely low discrimination at Step 3, varying between 7- and 90-fold (Kati *et al.*, 1992). This low discrimination at Step 3 results in HIV-1 RT having one of the lowest fidelities among replicative polymerases. The level of discrimination against incorrect nucleotides by HIV-1 RT is lower even than family Y polymerases, for example, yeast pol η, which

discriminates by a factor of 150, and also pol β, which discriminates between 85- and 2800-fold at Step 3 (Ahn *et al.*, 1997; Washington *et al.*, 2001). For both pol β (family X) and yeast pol η (family Y), elemental effects on nucleotide incorporation would indicate that the conformational change is rate limiting for both correct and incorrect nucleotide incorporation, although yeast pol η has a higher elemental effect during dNTP incorporation opposite certain DNA lesions (Washington *et al.*, 2001; Werneburg *et al.*, 1996), which may indicate that chemistry becomes rate limiting in certain cases. However, it has been suggested for the Dpo4 polymerase, another family Y member, that chemistry is rate limiting for incorrect nucleotide incorporation (Fiala and Suo, 2004a,b).

Experiments studying dNTP incorporation using 2-AP as a signal have expanded the details of nucleotide selection by pol β. Correct nucleotide incorporation by this enzyme shows two changes in fluorescence, a fast change followed by a slow one. The slow change corresponds to the quench-flow derived k_{pol} (Step 3), the rate-limiting step. The faster change is thought to correspond to an event occurring after dNTP-binding but before the conformational change has occurred (likely the crystallographically observed conformational transition affecting the fingers subdomain). The two fluorescent changes were also observed upon incorporation of incorrect nucleotides. The rate of the fastest change was of a similar value to that observed for correct nucleotide incorporation. However, the second phase is slowed dramatically (600-fold) compared with correct nucleotide incorporation (Zhong *et al.*, 1997). These experiments suggest that correct and incorrect nucleotide binding both induce the fast open-to-closed conformational transition affecting the fingers subdomain, and that discrimination occurs at a subsequent rate-limiting step, the molecular basis of which is still unclear.

In summary, all evidence so far points to the fact that discrimination takes place at a step occurring after the closing of the fingers domain. Kinetically, this step is rate limiting. Structurally, it is likely to correspond to the setting of the molecular stage leading to chemistry, which may include side-chain rearrangements, positioning of the various groups involved in catalysis, or other requirements to reach the transition state. When a correct nucleotide is provided, the setting of the chemical stage proceeds harmoniously, albeit at a rate-limiting pace. When an incorrect nucleotide is provided, the proper geometry of all active site components required for chemistry cannot be attained with the same degree of perfection, and thus the chemical step may become rate limiting. In any case, the setting of the stage is slower because all interactions required for chemistry are either prevented from being made or are made suboptimally.

VIII. Phosphoryl Transfer Reaction, Product Release, and Translocation of the Primer/Template DNA

A. *Phosphoryl Transfer Reaction and Product Release*

The mechanism of nucleotide addition by DNA polymerases was proposed on the basis of the nearly identical mechanism seen for the 3'-5' exonuclease of DNA polymerase I (Steitz, 1993, 1998). Briefly (because it has been reviewed extensively, e.g., in Steitz, 1998, and Li and Waksman, 2001b), the mechanism is proposed to occur as follows. Two metal ions (Mg^{2+}) are octahedrally coordinated by the triphosphate of an incoming nucleotide and side-chains in the active site. One metal (metal B) is ligated in the base of the octahedral plane by four oxygen atoms, contributed by the β- and γ-phosphates and two universally conserved carboxylate groups. The coordination sphere of the metal ion is completed on each side of the octahedral plane by interactions with oxygen atoms in the α-phosphate and the carbonyl oxygen of a Tyr residue. The other metal ion (metal A) is coordinated to the octahedral plane by oxygen atoms from the carboxylate of Asp 882 (Klenow fragment), the α-phosphate and two water molecules. On one side of the octahedral plane, metal A is ligated by an oxygen atom from the carboxylate of Asp 705 (Klenow fragment) and on the other side by the 3'-OH group of the ribose moiety on the primer strand. In the proposed mechanism, metal ion A lowers the affinity of the 3'OH for the hydrogen, facilitating the 3' O^- attack on the α-phosphate. Metal ion B assists the leaving of the PPi, and both metal ions stabilize the structure and charge of the expected pentacovalent transition state.

The phosphoryl transfer reaction is followed by a second conformational change, which allows the release of the PPi product (Step 5). Studying the reverse reaction, that is, pyrophosphorolysis for pol β with 2-AP fluorescence, showed three distinct fluorescence changes. The slowest phase corresponded to the rate of formation of dNTP, the product of pyrophosphorolysis, whereas the other two phases were thought to report on events happening before chemistry (Dunlap and Tsai, 2002; Zhong *et al.*, 1997).

It has been shown for the Klenow fragment that the PPi product has only a fivefold lower affinity for the E:p/t complex than dNTPs, suggesting that the product of the reaction could compete for binding of dNTPs (Kuchta *et al.*, 1987). However, for T7 DNA polymerase, the affinity of PPi is extremely low and is nowhere near comparable to affinities for correct nucleotide binding, differing by nearly a factor of 1000 (Patel *et al.*, 1991). T4 has similarly reduced affinities for PPi compared with Klenow, being in the low millimolar range (Capson *et al.*, 1992).

B. Translocation of Primer/Template DNA

In family A polymerases, translocation of the p/t DNA must occur coincidentally with the opening of the fingers subdomain. The Klentaq1 system provides an appropriate model to illustrate the motion and its consequences. We have mentioned the role of Tyr 671 which, in the open form of the fingers subdomain, stacks against the first base pair of the duplex part of the p/t DNA (Fig. 3C). In that position, Tyr 671 appears to position the p/t DNA in the appropriate register against the active site of the enzyme. In the closed form, Tyr 671 moves out to make room for the first templating base (Fig. 4C). Once a nucleotide has reacted to the 3'-OH primer strand, the opening of the fingers subdomain would bring Tyr 671 back and thus would risk a steric clash with the newly formed base pair unless the latter translocates. How this occurs is not known. However, it has been hypothesized that in the open state, the DNA is able to move along the ''electrostatic'' tunnel or cylinder formed by the DNA-binding site (mostly formed by the palm subdomain and the wrapping around of the thumb subdomain; see Section V; Guajardo and Sousa, 1997). Indeed, the DNA-binding site is ''coated'' by a strongly positive electrostatic field emanating from a large number of positively charged residues. In such an environment, interactions with the DNA may be interchangeable and thus, perhaps paradoxically, the DNA may be relatively free to move. Thus, at any given time, the newly formed base pair is present only a fraction of the time in the active site of the open complex. Thus, Tyr 671 can probe the environment around the newly formed base pair and insert itself on top of it when space allows, that is, when the p/t DNA has slid away from the active site. Packing of Tyr 671 against the newly formed base pair stabilizes the DNA in the proper register, and another cycle of nucleotide incorporation could be initiated.

C. Force Generation: DNA Polymerases as Molecular Motors

One of the most exciting developments in the field of DNA polymerases has been the use of single-molecule optical and magnetic traps and atomic force microscopes to study the behavior of DNA polymerases under the constraints of forces applied to the primer/template substrate. The T7 DNA polymerase was studied with an optical trap (Wuite *et al.*, 2000) while the Klenow fragment of *E. coli*, its 3'-5' exonuclease deficient mutant, and 3'-5' exonuclease deficient mutant of T7 polymerase were studied using a magnetic trap (Maier *et al.*, 2000). More recently, the behavior of single molecules of HIV1 RT was studied using atomic force microscopy (Lu *et al.*, 2004). These studies take advantage of progress made in single-molecule

manipulation of DNAs and use single-molecule assays based on the differential elasticity of single-stranded and double-stranded DNAs. The three sets of experiments showed similar behavior. These studies showed that the rate of the replication reaction catalyzed by DNA polymerases is altered when a force is applied to the template strand (Lu *et al.*, 2004; Maier *et al.*, 2000; Wuite *et al.*, 2000). It was observed that the replication rate decreases at high forces and appears to increase at low force. The ''stall'' force, the mechanical force that is necessary to apply to the stretched DNA to block DNA polymerization, varies but is within a range of 15–40 pN, a force that is considered ''large'' for molecular motors. These studies also point to the fact that the force load acts on the rate-limiting step identified kinetically, thereby indicating that the limiting (rate-determining) step involves work by the DNA polymerase and therefore motion against an external force. The molecular basis of this force-generating step is unknown, although most studies have argued (but not demonstrated) that the step affected by the force load applied to the DNA is the closing of the fingers domain. Such a suggestion has been borne out by a recent *in silico* study using molecular dynamics simulations (Andricioaei *et al.*, 2004). In this study, the Klentaq1 ternary complex of Li *et al.* (1998b) was subjected to an external force applied to the template DNA. It was shown that at a medium-to-high force regimen, the closing of the fingers domain appears to be most affected, thus arguing for a role of this conformational transition in the force-generating step. It appears therefore that, although the open-to-closed conformational transition affecting the fingers domain is unlikely to be the kinetically observed rate-limiting step (see Section VII), it may play an active role in motioning the DNA polymerase along the DNA. However, it is important to keep in mind that not everybody agrees with such a conclusion and that it has been argued there is no need to involve a force generation step to move DNA polymerases along the DNA as a fraying mechanism as described in Section VIII.B may be sufficient (Guajardo and Sousa, 1997). In that context, the force generated by the DNA polymerase would correspond to the indirect effect of a tightening of the polymerase around the DNA during the rate-limiting step following the closing of the fingers domain.

IX. Conclusion

The study of DNA polymerase function has experienced remarkable progress reflected in three phases. The first phase is marked by the discovery of DNA polymerases by Kornberg and colleagues (Kornberg *et al.*, 1956; Lehman *et al.*, 1958). This pioneering phase saw rapid advances in our understanding of DNA replication. The second phase was initiated by the structure of the Klenow fragment by Steitz and colleagues (Ollis

et al., 1985). This structure provided the basis for understanding the molecular basis of DNA polymerization and informed the conduct of research in this area. The third phase provided the details of the kinetic pathway of nucleotide incorporation by Benkovic and Johnson and their colleagues (Capson *et al.*, 1992; Dahlberg and Benkovic, 1991; Donlin *et al.*, 1991; Eger and Benkovic, 1992; Kati *et al.*, 1992; Kuchta *et al.*, 1987, 1988; Patel *et al.*, 1991; Wong *et al.*, 1991), demonstrating that the enzyme must cycle through a succession of states, some of which provide the readout necessary to discriminate against incorrect nucleotide incorporation. These papers have formed the basis for research in the polymerase field to this day. Notably, looming large in the horizon of the structural biology landscape was the capture of the ''rate-limiting'' step. This holy grail of structural biology appeared to have been attained in 1994 and 1998 with the remarkable succession of structural characterization of the E':p/t:ddNTP complexes for several DNA polymerases: these structures suggested that the rate-limiting step is caused by the closure of the fingers subdomain (Doublie *et al.*, 1998; Huang *et al.*, 1998; Kiefer *et al.*, 1998; Li *et al.*, 1998b; Pelletier *et al.*, 1994). However, this suggestion does not seem to hold very well over the passage of time. Evidence, albeit all indirect, has accumulated to suggest that, on the contrary, the captured E':p/t:ddNTP state may be that of a fast step preceding the rate-limiting conformational step, but not the rate-limiting step itself. In the next few years, research will head toward elucidating the nature of the rate-limiting step and providing the lacking details of the nucleotide incorporation cycle.

Acknowledgments

This work was funded by grant #067879 from the Wellcome Trust to GW.

References

Abbotts, J., Sen Gupta, D. N., Zmudzka, B., Widen, S. G., Notario, V., and Wilson, S. H. (1988). Expression of human DNA polymerase β in *Escherichia coli* and characterization of the recombinant enzyme. *Biochemistry* **27,** 901–909.

Ahn, J., Werneburg, B. G., and Tsai, M. D. (1997). DNA polymerase β: Structure-fidelity relationship from pre-steady-state kinetic analyses of all possible correct and incorrect base pairs for wild type and R283A mutant. *Biochemistry* **36,** 1100–1107.

Andricioaei, I., Goel, A., Herschbach, D., and Karplus, M. (2004). Dependence of DNA polymerase replication rate on external forces: A model based on molecular dynamics simulations. *Biophys. J.* **87,** 1478–1497.

Astatke, M., Grindley, N. D., and Joyce, C. M. (1995). Deoxynucleoside triphosphate and pyrophosphate binding sites in the catalytically competent ternary complex for the polymerase reaction catalyzed by DNA polymerase I (Klenow fragment). *J. Biol. Chem.* **270,** 1945–1954.

Basu, A., and Modak, M. J. (1987). Identification and amino acid sequence of the deoxynucleoside triphosphate binding site in *Escherichia coli* DNA polymerase I. *Biochemistry* **26,** 1704–1709.

Beese, L. S., Derbyshire, V., and Steitz, T. A. (1993a). Structure of DNA polymerase I Klenow fragment bound to duplex DNA. *Science* **260,** 352–355.

Beese, L. S., Friedman, J. M., and Steitz, T. A. (1993b). Crystal structures of the Klenow fragment of DNA polymerase I complexed with deoxynucleoside triphosphate and pyrophosphate. *Biochemistry* **32,** 14095–14101.

Bork, P., Hofmann, K., Bucher, P., Neuwald, A., Altschul, S., and Koonin, E. (1997). A superFamily of conserved domains in DNA damage-responsive cell cycle checkpoint proteins. *FASEB J.* **11,** 68–76.

Boudsocq, F., Iwai, S., Hanaoka, F., and Woodgate, R. (2001). *Sulfolobus solfataricus* P2 DNA polymerase IV (Dpo4): An archaeal DNA polymerase with lesion-bypass properties akin to eukaryotic pol η. *Nucleic Acids Res.* **15,** 4607–4613.

Braithwaite, D. K., and Ito, J. (1993). Compilation, alignment, and phylogenetic relationships of DNA polymerases. *Nucleic Acids Res.* **21,** 787–802.

Bruskov, V. I., and Poltev, V. I. (1979). On molecular mechanisms of nucleic acid synthesis. Fidelity aspects: 2. Contribution of protein-nucleotide recognition. *J. Theor. Biol.* **78,** 29–41.

Burgers, P. M., Koonin, E. V., Bruford, E., Blanco, L., Burtis, K. C., Christman, M. F., Copeland, W. C., Friedberg, E. C., Hanaoka, F., Hinkle, D. C., Lawrence, C. W., Nakanishi, M., Ohmori, H., Prakash, L., Prakash, S., Reynaud, C. A., Sugino, A., Todo, T., Wang, Z., Weill, J. C., and Woodgate, R. (2001). Eukaryotic DNA polymerases: Proposal for a revised nomenclature. *J. Biol. Chem.* **276,** 43487–43490.

Cann, I. K., Komori, K., Toh, H., Kanai, S., and Ishino, Y. (1998). A heterodimeric DNA polymerase: Evidence that members of Euryarchaeota possess a distinct DNA polymerase. *Proc. Natl. Acad. Sci. USA* **95,** 14250–14255.

Capson, T. L., Peliska, J. A., Kaboord, B. F., Frey, M. W., Lively, C., Dahlberg, M., and Benkovic, S. J. (1992). Kinetic characterization of the polymerase and exonuclease activities of the gene 43 protein of bacteriophage T4. *Biochemistry* **31,** 10984–10994.

Carroll, S. S., Cowaet, M., and Benkovic, S. J. (1991). A mutant of DNA polymerase I (Klenow Fragment) with reduced fidelity. *Biochemistry* **30,** 804–813.

Dahlberg, M. E., and Benkovic, S. J. (1991). Kinetic mechanism of DNA polymerase I (Klenow fragment): Identification of a second conformational change and evaluation of the internal equilibrium constant. *Biochemistry* **30,** 4835–4843.

Das, D., and Georgiadis, M. M. (2004). The crystal structure of the monomeric reverse transcriptase from Moloney murine leukemia virus. *Structure* **12,** 819–829.

Delarue, M., Poch, O., Tordo, N., Moras, D., and Argos, P. (1990). An attempt to unify the structure of polymerases. *Protein Eng.* **3,** 461–467.

Dianov, G. L., Sleeth, K. M., Dianova, II, and Allinson, S. L. (2003). Repair of abasic sites in DNA. *Mutat. Res.* **531,** 157–163.

Ding, J., Das, K., Hsiou, Y., Sarafianos, S. G., Clark, A. D., Jr., Jacobo-Molina, A., Tantillo, C., Hughes, S. H., and Arnold, E. (1998). Structure and functional implications of the polymerase active site region in a complex of HIV-1 RT with a double-stranded DNA template-primer and an antibody Fab fragment at 2.8 Å resolution. *J. Mol. Biol.* **284,** 1095–1111.

Ding, J., Das, K., Moereels, H., Koymans, L., Andries, K., Janssen, P. A., Hughes, S. H., and Arnold, E. (1995a). Structure of HIV-1 RT/TIBO R 86183 complex reveals similarity in the binding of diverse nonnucleoside inhibitors. *Nat. Struct. Biol.* **2,** 407–415.

Ding, J., Das, K., Tantillo, C., Zhang, W., Clark, A. D., Jr., Jessen, S., Lu, X., Hsiou, Y., Jacobo-Molina, A., Andries, K., Pauwels, R., Moereels, H., Koymans, L., Janssen, P. A. J., Smith, R. H., Jr., Kroeger Koepke, M., Michejda, C. J., Hughes, S. H., and Arnold, E. (1995b). Structure of HIV-1 reverse transcriptase in a complex with the non-nucleoside inhibitor alpha-APA R 95845 at 2.8 Å resolution. *Structure* **3,** 365–379.

Divita, G., Rittinger, K., Geourjon, C., Deleage, G., and Goody, R. S. (1995a). Dimerization kinetics of HIV-1 and HIV-2 reverse transcriptase: A two step process. *J. Mol. Biol.* **245,** 508–521.

Divita, G., Rittinger, K., Restle, T., Immendorfer, U., and Goody, R. S. (1995b). Conformational stability of dimeric HIV-1 and HIV-2 reverse transcriptases. *Biochemistry* **34,** 16337–16346.

Dominguez, O., Ruiz, J. F., Lain de Lera, T., Garcia-Diaz, M., Gonzalez, M. A., Kirchhoff, T., Martinez, A. C., Bernad, A., and Blanco, L. (2000). DNA polymerase μ (Pol μ), homologous to TdT, could act as a DNA mutator in eukaryotic cells. *EMBO J.* **19,** 1731–1742.

Dong, Q., Copeland, W. C., and Wang, T. S. (1993). Mutational studies of human DNA polymerase α: Identification of residues critical for deoxynucleotide binding and misinsertion fidelity of DNA synthesis. *J. Biol. Chem.* **268,** 24163–24174.

Donlin, M. J., Patel, S. S., and Johnson, K. A. (1991). Kinetic partitioning between the exonuclease and polymerase sites in DNA error correction. *Biochemistry* **30,** 538–546.

Doublie, S., Tabor, S., Long, A. M., Richardson, C. C., and Ellenberger, T. (1998). Crystal structure of a bacteriophage T7 DNA replication complex at 2.2 A resolution. *Nature* **391,** 251–258.

Dunlap, C. A., and Tsai, M. D. (2002). Use of 2-aminopurine and tryptophan fluorescence as probes in kinetic analyses of DNA polymerase β. *Biochemistry* **41,** 11226–11235.

Echols, H., and Goodman, M. F. (1991). Fidelity mechanism in DNA replication. *Annu. Rev. Biochem.* **60,** 477–511.

Eger, B. T., and Benkovic, S. J. (1992). Minimal kinetic mechanism for misincorporation by DNA polymerase I (Klenow fragment). *Biochemistry* **31,** 9227–9236.

Engel, J. D., and von Hippel, P. H. (1978). D(M6ATP) as a probe of the fidelity of base incorporation into polynucleotides by *Escherichia coli* DNA polymerase I. *J. Biol. Chem.* **253,** 935–939.

Eom, S. H., Wang, J., and Steitz, T. A. (1996). Structure of *Taq* ploymerase with DNA at the polymerase active site. *Nature* **382,** 278–281.

Esnouf, R., Ren, J., Ross, C., Jones, Y., Stammers, D., and Stuart, D. (1995). Mechanism of inhibition of HIV-1 reverse transcriptase by non-nucleoside inhibitors. *Nat. Struct. Biol.* **2,** 303–308.

Fiala, K. A., and Suo, Z. (2004a). Mechanism of DNA polymerization catalyzed by *Sulfolobus solfataricus* P2 DNA polymerase IV. *Biochemistry* **43,** 2116–2125.

Fiala, K. A., and Suo, Z. (2004b). Pre-steady-state kinetic studies of the fidelity of *Sulfolobus solfataricus* P2 DNA polymerase IV. *Biochemistry* **43,** 2106–2115.

Franklin, M. C., Wang, J., and Steitz, T. A. (2001). Structure of the replicating complex of a pol α Family DNA polymerase. *Cell* **105,** 657–667.

Freemont, P. S., Friedman, J. M., Beese, L. S., Sanderson, M. R., and Steitz, T. A. (1988). Cocrystal structure of an editing complex of Klenow fragment with DNA. *Proc. Natl. Acad. Sci. USA* **85,** 8924–8928.

Frey, M. W., Sowers, L. C., Millar, D. P., and Benkovic, S. J. (1995). The nucleotide analog 2-aminopurine as a spectroscopic probe of nucleotide incorporation by the Klenow fragment of *Escherichia coli* polymerase I and bacteriophage T4 DNA polymerase. *Biochemistry* **34,** 9185–9192.

Friedberg, E. C., Feaver, W. J., and Gerlach, V. L. (2000). The many faces of DNA polymerases: Strategies for mutagenesis and for mutational avoidance. *Proc. Natl. Acad. Sci. USA* **97,** 5681–5683.

Friedberg, E. C., and Gerlach, V. L. (1999). Novel DNA polymerases offer clues to the molecular basis of mutagenesis. *Cell* **98,** 413–416.

Garcia-Diaz, M., Dominguez, O., Lopez-Fernandez, L. A., de Lera, L. T., Saniger, M. L., Ruiz, J. F., Parraga, M., Garcia-Ortiz, M. J., Kirchhoff, T., and del Mazo, J. (2000). DNA polymerase λ (Pol λ), a novel eukaryotic DNA polymerase with a potential role in meiosis. *J. Mol. Biol.* **301,** 851–867.

Gillin, F. D., and Nossal, N. G. (1976). Control of mutation frequency by bacteriophage T4 DNA polymerase: II. Accuracy of nucleotide selection by the L88 mutator, CB120 antimutator, and wild type phage T4 DNA polymerases. *J. Biol. Chem.* **251,** 5225–5232.

Goodman, M. F., and Tippin, B. (2000). Sloppier copier DNA polymerases involved in genome repair. *Curr. Opin. Genet. Dev.* **10,** 162–168.

Gotte, M., Li, X., and Wainberg, M. A. (1999). HIV-1 reverse transcription: A brief overview focused on structure-function relationships among molecules involved in initiation of the reaction. *Arch. Biochem. Biophys.* **365,** 199–210.

Greider, C. W., and Blackburn, E. H. (1985). Identification of a specific telomere terminal transferase activity in *Tetrahymena* extracts. *Cell* **43,** 405–413.

Greider, C. W., and Blackburn, E. H. (1989). A telomeric sequence in the RNA of *Tetrahymena* telomerase required for telomere repeat synthesis. *Nature* **337,** 331–337.

Guajardo, R., and Sousa, R. (1997). A model for the mechanism of polymerase translocation. *J. Mol. Biol.* **265,** 8–19.

Hashimoto, H., Nishioka, M., Fujiwara, S., Takagi, M., Imanaka, T., Inoue, T., and Kai, Y. (2001). Crystal structure of DNA polymerase from hyperthermophilic archaeon *Pyrococcus kodakaraensis* KOD1. *J. Mol. Biol.* **306,** 469–477.

Hogg, M., Wallace, S. S., and Doublie, S. (2004). Crystallographic snapshots of a replicative DNA polymerase encountering an abasic site. *EMBO J.* **23,** 1483–1493.

Hopfner, K. P., Eichinger, A., Engh, R. A., Laue, F., Ankenbauer, W., Huber, R., and Angerer, B. (1999). Crystal structure of a thermostable type B DNA polymerase from *Thermococcus gorgonarius. Proc. Natl. Acad. Sci. USA* **96,** 3600–3605.

Hsieh, J. C., Zinnen, S., and Modrich, P. (1993). Kinetic mechanism of the DNA-dependent DNA polymerase activity of human immunodeficiency virus reverse transcriptase. *J. Biol. Chem.* **268,** 24607–24613.

Hsiou, Y., Ding, J., Das, K., Clark, A. D., Jr., Hughes, S. H., and Arnold, E. (1996). Structure of unliganded HIV-1 reverse transcriptase at 2.7 Å resolution: Implications of conformational changes for polymerization and inhibition mechanisms. *Structure* **4,** 853–860.

Huang, H., Chopra, R., Verdine, G. L., and Harrison, S. C. (1998). Structure of a covalently trapped catalytic complex of HIV-1 reverse transcriptase: Implications for drug resistance. *Science* **282,** 1669–1675.

Ito, J., and Braithwaite, D. K. (1991). Compilation and alignment of DNA polymerase sequences. *Nucl. Acids Res.* **19,** 4045–4057.

Jacobo-Molina, A., Ding, J., Nanni, R. G., Clark, A. D., Jr., Lu, X., Tantillo, C., Williams, R. L., Kamer, G., Ferris, A. L., Clark, P., Hizi, A., Hughes, S. H., and Arnold, E. (1993). Crystal structure of human immunodeficiency virus type 1 reverse transcriptase complexed with double-stranded DNA at 3.0 Å resolution shows bent DNA. *Proc. Natl. Acad. Sci. USA* **90,** 6320–6324.

Jaeger, J., Restle, T., and Steitz, T. A. (1998). The structure of HIV-1 reverse transcriptase complexed with an RNA pseudoknot inhibitor. *EMBO J.* **17,** 4535–4542.

Jezewska, M. J., Galletto, R., and Bujalowski, W. (2002). Dynamics of gapped DNA recognition by human polymerase *β*. *J. Biol. Chem.* **277,** 20316–20327.

Jezewska, M. J., Rajendran, S., and Bujalowski, W. (2001a). Energetics and specificity of Rat DNA polymerase *β* interactions with template-primer and gapped DNA substrates. *J. Biol. Chem.* **276,** 16123–16136.

Jezewska, M. J., Rajendran, S., and Bujalowski, W. (2001b). Interactions of the 8-kDa domain of rat DNA polymerase *β* with DNA. *Biochemistry* **40,** 3295–3307.

Johnson, R. E., Washington, M. T., Prakash, S., and Prakash, L. (1999). Bridging the gap: A family of novel DNA polymerases that replicate faulty DNA. *Proc. Natl. Acad. Sci. USA* **96,** 12224–12226.

Joyce, C. M., and Steitz, T. A. (1994). Function and structure relationships in DNA polymerases. *Annu. Rev. Biochem.* **63,** 777–822.

Kati, W. M., Johnson, K. A., Jerva, L. F., and Anderson, K. S. (1992). Mechanism and fidelity of HIV reverse transcriptase. *J. Biol. Chem.* **267,** 25988–25997.

Kelman, Z., and O'Donnell, M. (1995). DNA polymerase III holoenzyme: Structure and function of a chromosomal replicating machine. *Ann. Rev. Biochem.* **64,** 171–200.

Kensch, O., Restle, T., Wöhrl, B. M., Goody, R. S., and Steinhoff, H. J. (2000). Temperature-dependent equilibrium between the open and closed conformation of the p66 subunit of HIV-1 reverse transcriptase revealed by site-directed spin labelling. *J. Mol. Biol.* **301,** 1029–1039.

Kiefer, J. R., Mao, C., Braman, J. C., and Beese, L. S. (1998). Visualizing DNA replication in a catalytically active Bacillus DNA polymerase crystal. *Nature* **391,** 304–307.

Kim, S. J., Beard, W. A., Harvey, J., Shock, D. D., Knutson, J. R., and Wilson, S. H. (2003). Rapid segmental and subdomain motions of DNA polymerase *β*. *J. Biol. Chem.* **278,** 5072–5081.

Kim, Y., Eom, S. H., Wang, J., Lee, D. S., Suh, S. W., and Steitz, T. A. (1995). Crystal structure of *Thermus aquaticus* DNA polymerase. *Nature* **376,** 612–616.

Klenow, H., and Overgaard-Hansen, K. (1970). Proteolytic cleavage of DNA polymerase from *Escherichia coli* B into an exonuclease unit and a polymerase unit. *FEBS Lett.* **6,** 25–27.

Kohlstaedt, L. A., Wang, J., Friedman, J. M., Rice, P. A., and Steitz, T. A. (1992). Crystal structure at 3.5 A resolution of HIV-1 reverse transcriptase complexed with an inhibitor. *Science* **256,** 1783–1790.

Kornberg, A. (1980). ''DNA Replication.'' W. H. Freeman, San Francisco.

Kornberg, A., and Baker, T. A. (1992). ''DNA Replication.'' W. H. Freeman, New York.

Kornberg, A., Lehman, I. R., Bessman, M. J., and Simms, E. S. (1956). Enzymic synthesis of deoxyribonucleic acid. *Biochim. Biophys. Acta* **21,** 197–198.

Korolev, S., Nayal, M., Barnes, W. M., Di Cera, E., and Waksman, G. (1995). Crystal structure of the large fragment of *Thermus aquaticus* DNA polymerase I at 2.5 A resolution: Structural basis for thermostability. *Proc. Natl. Acad. Sci. USA* **92,** 9264–9268.

Krahn, J. M., Beard, W. A., Miller, H., Grollman, A. P., and Wilson, S. H. (2003). Structure of DNA polymerase β with the mutagenic DNA lesion 8-oxodeoxyguanine reveals structural insights into its coding potential. *Structure* **11,** 121–127.

Kraynov, V. S., Werneburg, B. G., Zhong, X., Lee, H., Ahn, J., and Tsai, M. D. (1997). DNA polymerase β: Analysis of the contributions of tyrosine-271 and asparagine-279 to substrate specificity and fidelity of DNA replication by pre-steady-state kinetics. *Biochem. J.* **323,** 103–111.

Kuchta, R. D., Benkovic, P., and Benkovic, S. J. (1988). Kinetic mechanism whereby DNA polymerase I (Klenow) replicates DNA with high fidelity. *Biochemistry* **27,** 6716–6725.

Kuchta, R. D., Mizrahi, V., Benkovic, P. A., Johnson, K. A., and Benkovic, S. J. (1987). Kinetic mechanism of DNA polymerase I (Klenow). *Biochemistry* **26,** 8410–8417.

Kumar, A., Abbotts, J., Karawya, E. M., and Wilson, S. H. (1990). Identification and properties of the catalytic domain of mammalian DNA polymerase β. *Biochemistry* **29,** 7156–7159.

Lehman, I. R., Zimmerman, S. B., Adler, J., Bessman, M. J., Simms, E. S., and Kornberg, A. (1958). Enzymatic synthesis of deoxyribonucleic acid: V. Chemical composition of enzymatically synthesized deoxyribonucleic acid. *Proc. Natl. Acad. Sci. USA* **44,** 1191–1196.

Li, Y., Dutta, S., Doublie, S., Bdour, H. M., Taylor, J. S., and Ellenberger, T. (2004). Nucleotide insertion opposite a cis-syn thymine dimer by a replicative DNA polymerase from bacteriophage T7. *Nat. Struct. Mol. Biol.* **11,** 784–790.

Li, Y., Kong, Y., Korolev, S., and Waksman, G. (1998a). Crystal structures of the Klenow fragment of *Thermus aquaticus* DNA polymerase I complexed with deoxyribonucleoside triphosphates. *Protein Sci.* **7,** 1116–1123.

Li, Y., Korolev, S., and Waksman, G. (1998b). Crystal structures of open and closed forms of binary and ternary complexes of the large fragment of *Thermus aquaticus* DNA polymerase I: Structural basis for nucleotide incorporation. *EMBO J.* **17,** 7514–7525.

Li, Y., and Waksman, G. (2001a). Crystal structures of a ddATP-, ddTTP-, ddCTP-, and ddGTP-trapped ternary complex of Klentaq1: Insights into the nucleotide incorporation and selectivity. *Protein Sci.* **10,** 1225–1233.

Li, Y., and Waksman, G. (2001b). Structural studies of the Klentaq1 DNA polymerase. *Curr. Organic Chem.* **5,** 871–883.

Lin, T. C., Karam, G., and Konigsberg, W. H. (1994). Isolation, characterization, and kinetic properties of truncated forms of T4 DNA polymerase that exhibit 3'-5' exonuclease activity. *J. Biol. Chem.* **269,** 19286–19294.

Ling, H., Boudsocq, F., Plosky, B. S., Woodgate, R., and Yang, W. (2003). Replication of a cis-syn thymine dimer at atomic resolution. *Nature* **424,** 1083–1087.

Ling, H., Boudsocq, F., Woodgate, R., and Yang, W. (2001). Crystal structure of a Y-Family DNA polymerase in action: A mechanism for error-prone and lesion-bypass replication. *Cell* **107,** 91–102.

Ling, H., Sayer, J. M., Plosky, B. S., Yagi, H., Boudsocq, F., Woodgate, R., Jerina, D. M., and Yang, W. (2004). Crystal structure of a benzo[a]pyrene diol epoxide adduct in a ternary complex with a DNA polymerase. *Proc. Natl. Acad. Sci. USA* **101,** 2265–2269.

Loeb, L. A., and Kunkel, T. A. (1982). Fidelity of DNA synthesis. *Ann. Rev. Biochem.* **52,** 429–447.

Lu, H., Macosko, J., Habel-Rodriguez, D., Keller, R. W., Brozik, J. A., and Keller, D. J. (2004). Closing of the fingers domain generates motor forces in the HIV reverse transcriptase. *J. Biol. Chem.,* **279,** 54529–54532.

Madrid, M., Jacobo-Molina, A., Ding, J., and Arnold, E. (1999). Major subdomain rearrangement in HIV-1 reverse transcriptase simulated by molecular dynamics. *Proteins* **35,** 332–337.

Maier, D., Bensimon, D., and Croquette, V. (2000). Replication by a single DNA polymerase of a stretched single-stranded DNA. *Proc. Natl. Acad. Sci. USA* **97,** 12002–12007.

Martins, A., Ribeiro, G., Marques, M. I., and Costa, J. V. (1994). Genetic identification and nucleotide sequence of the DNA polymerase gene of African swine fever virus. *Nucleic Acids Res.* **22,** 208–213.

Matsumoto, Y., and Bogenhagen, D. F. (1991). Repair of a synthetic abasic site involves concerted reactions of DNA synthesis followed by excision and ligation. *Mol. Cell. Biol.* **11,** 4441–4447.

Matsumoto, Y., and Kim, K. (1995). Excision of deoxyribose phosphate residues by DNA polymerase β during DNA repair. *Science* **269,** 699–702.

Nair, D. T., Johnson, R. E., Prakash, S., Prakash, L., and Aggarwal, A. K. (2004). Replication by human DNA polymerase-ι occurs by Hoogsteen base-pairing. *Nature* **430,** 377–380.

Ollis, D. L., Brick, P., Hamlin, R., Xuong, N. G., and Steitz, T. A. (1985). Structure of large fragment of *Escherichia coli* DNA polymerase I complexed with dTMP. *Nature* **313,** 762–766.

Pata, J. D., Stirtan, W. G., Goldstein, S. W., and Steitz, T. A. (2004). Structure of HIV-1 reverse transcriptase bound to an inhibitor active against mutant reverse transcriptases resistant to other nonnucleoside inhibitors. *Proc. Natl. Acad. Sci. USA* **101,** 10548–10553.

Patel, S. S., Wong, I., and Johnson, K. A. (1991). Pre-steady-state kinetic analysis of processive DNA replication including complete characterization of an exonuclease-deficient mutant. *Biochemistry* **30,** 511–525.

Pavlov, A. R., and Karam, J. D. (1994). Binding specificity of T4 DNA polymerase to RNA. *J. Biol. Chem.* **269,** 12968–12972.

Pelletier, H., Sawaya, M. R., Kumar, A., Wilson, S. H., and Kraut, J. (1994). Structures of ternary complexes of rat DNA polymerase β, a DNA template-primer, and ddCTP. *Science* **264,** 1891–1903.

Pelletier, H., Sawaya, M. R., Wolfle, W., Wilson, S. H., and Kraut, J. (1996). Crystal structures of human DNA polymerase β complexed with DNA: Implications for catalytic mechanism, processivity, and fidelity. *Biochemistry* **35,** 12742–12761.

Petruska, J., Sowers, L. C., and Goodman, M. F. (1986). Comparison of nucleotide interactions in water, proteins, and vacuum: Model for DNA polymerase fidelity. *Proc. Natl. Acad. Sci. USA* **83,** 1559–1562.

Prasad, R., Widen, S., Singhal, R., Watkins, J., Prakash, L., and Wilson, S. (1993). Yeast open reading frame YCR14C encodes a DNA β-polymerase-like enzyme. *Nucl. Acids Res.* **21,** 5301–5307.

Purohit, V., Grindley, N. D., and Joyce, C. M. (2003). Use of 2-aminopurine fluorescence to examine conformational changes during nucleotide incorporation by DNA polymerase I (Klenow fragment). *Biochemistry* **42,** 10200–10211.

Rajendran, S., Jezewska, M. J., and Bujalowski, W. (1998). Human DNA polymerase β recognizes single-stranded DNA using two different binding modes. *J. Biol. Chem.* **273,** 31021–31031.

Rajendran, S., Jezewska, M. J., and Bujalowski, W. (2001). Recognition of template-primer and gapped DNA substrates by the human DNA polymerase β. *J. Mol. Biol.* **308,** 477–500.

Ren, J., Bird, L. E., Chamberlain, P. P., Stewart-Jones, G. B., Stuart, D. I., and Stammers, D. K. (2002). Structure of HIV-2 reverse transcriptase at 2.35-Å resolution and the mechanism of resistance to non-nucleoside inhibitors. *Proc. Natl. Acad. Sci. USA* **99,** 14410–14415.

Ren, J., Esnouf, R., Garman, E., Somers, D., Ross, C., Kirby, I., Keeling, J., Darby, G., Jones, Y., and Stuart, D. (1995). High resolution structures of HIV-1 RT from four RT-inhibitor complexes. *Nat. Struct. Biol.* **2,** 293–302.

Ren, J., Esnouf, R. M., Hopkins, A. L., Warren, J., Balzarini, J., Stuart, D. I., and Stammers, D. K. (1998). Crystal structures of HIV-1 reverse transcriptase in complex with carboxanilide derivatives. *Biochemistry* **37,** 14394–14403.

Ren, J., Nichols, C. E., Chamberlain, P. P., Weaver, K. L., Short, S. A., and Stammers, D. K. (2004). Crystal structures of HIV-1 reverse transcriptases mutated at codons 100, 106 and 108 and mechanisms of resistance to non-nucleoside inhibitors. *J. Mol. Biol.* **336,** 569–578.

Rittinger, K., Divita, G., and Goody, R. S. (1995). Human immunodeficiency virus reverse transcriptase substrate-induced conformational changes and the mechanism of inhibition by nonnucleoside inhibitors. *Proc. Natl. Acad. Sci. USA* **92,** 8046–8049.

Rodgers, D. W., Gamblin, S. J., Harris, B. A., Ray, S., Culp, J. S., Hellmig, B., Woolf, D. J., Debouck, C., and Harrison, S. C. (1995). The structure of unliganded reverse transcriptase from the human immunodeficiency virus type 1. *Proc. Natl. Acad. Sci. USA* **92,** 1222–1226.

Rodriguez, A. C., Park, H. W., Mao, C., and Beese, L. S. (2000). Crystal structure of a pol α Family DNA polymerase from the hyperthermophilic archaeon *Thermococcus* sp. 9 degrees N-7. *J. Mol. Biol.* **299,** 447–462.

Roth, M. J., Tanese, N., and Goff, S. P. (1985). Purification and characterization of murine retroviral reverse transcriptase expressed in *Escherichia coli*. *J. Biol. Chem.* **260,** 9326–9335.

Rothwell, P. J., Berger, S., Kensch, O., Felekyan, S., Antonik, M., Wohrl, B. M., Restle, T., Goody, R. S., and Seidel, C. A. (2003). Multiparameter single-molecule fluorescence spectroscopy reveals heterogeneity of HIV-1 reverse transcriptase:primer/template complexes. *Proc. Natl. Acad. Sci. USA* **100,** 1655–1660.

Sarafianos, S. G., Clark, A. D., Jr., Das, K., Tuske, S., Birktoft, J. J., Ilankumaran, P., Ramesha, A. R., Sayer, J. M., Jerina, D. M., Boyer, P. L., Hughes, S. H., and Arnold, E. (2002). Structures of HIV-1 reverse transcriptase with pre- and post-translocation AZTMP-terminated DNA. *EMBO J.* **21,** 6614–6624.

Sarafianos, S. G., Das, K., Tantillo, C., Clark, A. D., Jr., Ding, J., Whitcomb, J. M., Boyer, P. L., Hughes, S. H., and Arnold, E. (2001). Crystal structure of HIV-1 reverse transcriptase in complex with a polypurine tract RNA:DNA. *EMBO J.* **20,** 1449–1461.

Sawaya, M. R., Pelletier, H., Kumar, A., Wilson, S. H., and Kraut, J. (1994). Crystal structure of rat DNA polymerase β: Evidence for a common polymerase mechanism. *Science* **264,** 1930–1935.

Sawaya, M. R., Prasad, R., Wilson, S. H., Kraut, J., and Pelletier, H. (1997). Crystal structures of human DNA polymerase β complexed with gapped and nicked DNA: Evidence for an induced fit mechanism. *Biochemistry* **36,** 11205–11215.

Shah, A. M., Maitra, M., and Sweasy, J. B. (2003). Variants of DNA polymerase β extend mispaired DNA due to increased affinity for nucleotide substrate. *Biochemistry* **42,** 10709–10717.

Silvian, L. F., Toth, E. A., Pham, P., Goodman, M. F., and Ellenberger, T. (2001). Crystal structure of a DinB Family error-prone DNA polymerase from *Sulfolobus solfataricus*. *Nat. Struct. Biol.* **8,** 984–989.

Sloane, D. L., Goodman, M. F., and Echols, H. (1988). The fidelity of base selection by the polymerase subunit of DNA polymerase III holoenzyme. *Nucleic Acids Res.* **16,** 6465–6475.

Sluis-Cremer, N., Arion, D., and Parniak, M. A. (2000). Molecular mechanisms of HIV-1 resistance to nucleoside reverse transcriptase inhibitors (NRTIs). *Cell Mol. Life Sci.* **57,** 1408–1422.

Smerdon, S. J., Jager, J., Wang, J., Kohlstaedt, L. A., Chirino, A. J., Friedman, J. M., Rice, P. A., and Steitz, T. A. (1994). Structure of the binding site for nonnucleoside inhibitors of the reverse transcriptase of human immunodeficiency virus type 1. *Proc. Natl. Acad. Sci. USA* **91,** 3911–3915.

Steitz, T. A. (1993). DNA- and RNA-dependent DNA polymerases. *Curr. Opin. Struct. Biol.* **3,** 31–38.

Steitz, T. A. (1994). A unified polymerase mechanism for nonhomologous DNA and RNA polymerases. *Science* **266,** 2022–2026.

Steitz, T. A. (1998). A mechanism for all polymerases. *Nature* **391,** 231–232.

Suzuki, M., Baskin, D., Hood, L., and Loeb, L. A. (1996). Random mutagenesis of *Thermus aquaticus* DNA polymerase I: Concordance of immutable sites *in vivo* with the crystal structure. *Proc. Natl. Acad. Sci. USA* **93,** 9670–9675.

Tabor, S., Huber, H. E., and Richardson, C. C. (1987). *Escherichia coli* thioredoxin confers processivity on the DNA polymerase activity of the gene 5 protein of bacteriophage T7. *J. Biol. Chem.* **262,** 16212–16223.

Topal, M. D., Di Guiseppi, S. R., and Sinha, N. K. (1980). Molecular basis for substitution mutations: Effect of primer terminal and template residues on nucleotide selection by phage T4 DNA polymerase *in vitro*. *J. Biol. Chem.* **255,** 11717–11724.

Trincao, J., Johnson, R. E., Escalante, C. R., Prakash, S., Prakash, L., and Aggarwal, A. K. (2001). Structure of the catalytic core of *S. cerevisiae* DNA polymerase η: Implications for translesion DNA synthesis. *Mol. Cell* **8,** 417–426.

Tuerk, C., Eddy, S., Parma, D., and Gold, L. (1990). Autogenous translational operator recognized by bacteriophage T4 DNA polymerase. *J. Mol. Biol.* **213,** 749–761.

Uemori, T., Sato, Y., Doi, H., and Ishino, Y. (1997). A novel DNA polymerase in the hyperthermophilic acrhaeon, *Pyrococcus furiosus*: Gene cloning, expression and characterization. *Genes to Cell* **2,** 499–512.

Uljon, S. N., Johnson, R. E., Edwards, T. A., Prakash, S., Prakash, L., and Aggarwal, A. K. (2004). Crystal structure of the catalytic core of human DNA polymerase κ. *Structure* **12,** 1395–1404.

Vande Berg, B. J., Beard, W. A., and Wilson, S. H. (2001). DNA structure and aspartate 276 influence nucleotide binding to human DNA polymerase β. Implication for the identity of the rate-limiting conformational change. *J. Biol. Chem.* **276,** 3408–3416.

Wang, C. C., Pavlov, A., and Karam, J. D. (1997a). Evolution of RNA-binding specificity in T4 DNA polymerase. *J. Biol. Chem.* **272,** 17703–17710.

Wang, J., Sattar, A. K., Wang, C. C., Karam, J. D., Konigsberg, W. H., and Steitz, T. A. (1997b). Crystal structure of a pol α Family replication DNA polymerase from bacteriophage RB69. *Cell* **89,** 1087–1099.

Washington, M. T., Prakash, L., and Prakash, S. (2001). Yeast DNA polymerase η utilizes an induced-fit mechanism of nucleotide incorporation. *Cell* **107,** 917–927.

Watson, J. D., and Crick, F. H. (1953a). Genetical implications of the structure of deoxyribonucleic acid. *Nature* **171,** 964–967.

Watson, J. D., and Crick, F. H. (1953b). Molecular structure of nucleic acids: A structure for deoxyribose nucleic acid. *Nature* **171,** 737–738.

Werneburg, B. G., Ahn, J., Zhong, X., Hondal, R. J., Kraynov, V. S., and Tsai, M. D. (1996). DNA polymerase β: Pre-steady-state kinetic analysis and roles of arginine–283 in catalysis and fidelity. *Biochemistry* **35,** 7041–7050.

Wöhrl, B. M., Krebs, R., Goody, R. S., and Restle, T. (1999). Refined model for primer/template binding by HIV-1 reverse transcriptase: Pre-steady-state kinetic analyses of primer/template binding and nucleotide incorporation events distinguish between different binding modes depending on the nature of the nucleic acid substrate. *J. Mol. Biol.* **292,** 333–344.

Wong, I., Patel, S. S., and Johnson, K. A. (1991). An induced-fit kinetic mechanism for DNA replication fidelity: Direct measurement by single-turnover kinetics. *Biochemistry* **30,** 526–537.

Woodgate, R. (1999). A plethora of lesion-replicating DNA polymerases. *Genes Dev.* **13,** 2191–2195.

Wuite, G. J. L., Smith, S. B., Young, M., Keller, D., and Bustamante, C. (2000). Single-molecule studies of the effect of template tension on T7 DNA polymerase activity. *Nature* **404,** 103–106.

Yang, G., Franklin, M., Li, J., Lin, T. C., and Konigsberg, W. (2002a). Correlation of the kinetics of finger domain mutants in RB69 DNA polymerase with its structure. *Biochemistry* **41,** 2526–2534.

Yang, L., Arora, K., Beard, W. A., Wilson, S. H., and Schlick, T. (2004). Critical role of magnesium ions in DNA polymerase β's closing and active site assembly. *J. Am. Chem. Soc.* **126,** 8441–8453.

Yang, L., Beard, W. A., Wilson, S. H., Broyde, S., and Schlick, T. (2002b). Polymerase β simulations suggest that Arg258 rotation is a slow step rather than large subdomain motions per se. *J. Mol. Biol.* **317,** 651–671.

Yang, W. (2003). Damage repair DNA polymerases Y. *Curr. Opin. Struct. Biol.* **13,** 23–30.

Zhao, Y., Jeruzalmi, D., Moarefi, I., Leighton, L., Lasken, R., and Kuriyan, J. (1999). Crystal structure of an archaebacterial DNA polymerase. *Structure Fold Des.* **7,** 1189–1199.

Zhong, X., Patel, S. S., Werneburg, B. G., and Tsai, M. D. (1997). DNA polymerase β: Multiple conformational changes in the mechanism of catalysis. *Biochemistry* **36,** 11891–11900.

Zhou, B. L., Pata, J. D., and Steitz, T. A. (2001). Crystal structure of a DinB lesion bypass DNA polymerase catalytic fragment reveals a classic polymerase catalytic domain. *Mol. Cell* **8,** 427–437.